J. Fluid Mech. (1990), *vol.* 216, *pp.* 255–284
Printed in Great Britain

An airfoil theory of bifurcating laminar separation from thin obstacles

By C. J. LEE AND H. K. CHENG

Department of Aerospace Engineering, University of Southern California, Los Angeles, CA 90089-1191, USA

(Received 12 September 1988 and in revised form 11 December 1989)

Global interaction of the boundary layer separating from an obstacle with resulting open/closed wakes is studied for a thin airfoil in a steady flow. Replacing the Kutta condition of the classical theory is the breakaway criterion of the laminar triple-deck interaction (Sychev 1972; Smith 1977), which, together with the assumption of a uniform wake/eddy pressure, leads to a nonlinear equation system for the breakaway location and wake shape. The solutions depend on a Reynolds number Re and an airfoil thickness ratio or incidence τ and, in the domain $Re^{\frac{1}{16}}\tau = O(1)$ considered, the separation locations are found to be far removed from the classical Brillouin–Villat point for the breakaway from a smooth shape. Bifurcations of the steady-state solution are found among examples of symmetrical and asymmetrical flows, allowing open and closed wakes, as well as symmetry breaking in an otherwise symmetrical flow. Accordingly, the influence of thickness and incidence, as well as Reynolds number is critical in the vicinity of branch points and cut-off points where steady-state solutions can/must change branches/types. The study suggests a correspondence of this bifurcation feature with the lift hysteresis and other aerodynamic anomalies observed from wind-tunnel and numerical studies in subcritical and high-subcritical Re flows.

1. Introduction

In spite of the great success in hydrodynamic theory brought about by the Kutta–Joukowski condition (Lamb 1932; Sedov 1965; Batchelor 1967), a fully attached flow on the aero/hydrofoil in a real fluid may still be considered an exception to the rule. Students of theoretical aerodynamics are all the more disappointed when they attempt to reconcile aerodynamic analysis with the boundary-layer theory and with experiments, especially for (chord) Reynolds numbers in the range $Re = 10^2$–10^5 (see for example, Schmitz 1942; Althaus 1980; Mueller 1979, 1985). The inadequacy of the classical analysis clearly results from the lack of an interaction mechanism relating the boundary layer with its outer flow, and also from the steady-state assumption taken for granted in most studies. The present work will nevertheless be limited mainly to the global interaction problem in a *steady* flow resulting from laminar separation.

Without taking the unsteady features into consideration, the applicability of the theory to aero/hydronautics must be very limited, inasmuch as a separated flow is believed to be inherently unstable, and most aerodynamic measurements can furnish only the time- or the conditionally averaged unsteady data. The steady-state analysis is undertaken here, nevertheless, as an answer to a basic issue in theoretical aerodynamics: whether a steady separated flow may represent an asymptotic

solution to the Navier–Stokes equations (in the limit $Re \to \infty$) beyond the stage of the classical boundary-layer breakdown (Goldstein 1948; Stewartson 1958), or simply as an alternative to an unseparated flow with a fully attached boundary layer (under the same flow conditions). A feature brought out by the present study is the multiplicity of the steady states which can occur in certain parts of the unit-order $Re^{\frac{1}{16}}\tau$ domain, which may explain hysteresis and certain aerodynamic anomalies occurring in subcritical flows.

1.1. *Flow hysteresis and non-uniqueness examples*

The results suggest a correspondence between the steady-state bifurcation and lift hysteresis commonly observed in low-Re flow, and that the steady-state bifurcation can occur in a strictly subcritical-Re flow. For a symmetric body/airfoil, the bifurcation can take the special form of symmetry breaking, generating lift on a symmetric airfoil at zero angle of attack, rather similar to the anomaly observed experimentally for thick profiles in the high subcritical Re-range (see figure 1 taken from Athaus 1980; also refer Schewe 1983). From the viewpoint of flow instability, the study should be useful in yielding a structure of the non-parallel flows, to which questions of global instability/receptivity (Morkovin & Paranjape 1971; Goldstein 1984) as well as wake breakdown (Brown, Cheng & Smith 1988) can be addressed.

The triple-deck theory, which provides the key element of the present analysis, allows the boundary layer and its outer flow to interact in such a way as to render upstream influence and local separation possible. The formalism has been established through seminal works of Stewartson (1969), Neiland (1969), Messiter (1970) and others; the literature of its subsequent development is extensive (see reviews by Stewartson 1974, 1981; Messiter 1978, 1983; Smith 1982, 1986 and Sychev 1987). Sychev (1972) recognized that a triple deck on a smooth obstacle can produce a self-induced, local pressure gradient large enough for the laminar boundary layer to *breakaway* from the surface and to support a global (body-scale) wake structure consistent with Kirchhoff's (1869) model of an open wake. Sychev's penetrating analysis was substantiated by Smith (1977, 1979) who solved numerically the reduced lower-deck problem and provided additional details for several regions of the wake interior. Certain key features in Smith's study, including the length and height of a thin eddy far downstream of the obstacle, draw some support from a series of steady-state Navier–Stokes solutions computed by Fornberg (1980) for $Re \leqslant 400$, although the agreement is far from perfect. There also remain unsettled difficulties in the asymptotic theory with the closure problem of the main eddy far downstream (Smith 1979). However, an alternative to this global structure, featuring a giant eddy of unit-order aspect ratio and a cuspidal closure (as in Sadovskii 1971 and Peregrine 1985), appears also to be mathematically admissible. Indeed, numerical solutions carried out by Fornberg (1985) to a Re-range higher than 400 indicate a strong preference for this alternative; its likelihood has been substantiated to considerable detail in a subsequent study by Smith (1985), adopting the large-eddy model just mentioned. To be sure, the theoretical problem posed in these studies stipulates a symmetric flow pattern which could be realized only with the help of a splitter plate (endowed with a frictionless surface). Even if the Fornberg–Smith (1985) model could be accepted as a viable conjecture, the proposal does not rule out the thin-eddy model (Smith 1977, 1979) as its alternative, by virtue of the possible non-uniqueness-solution bifurcation.

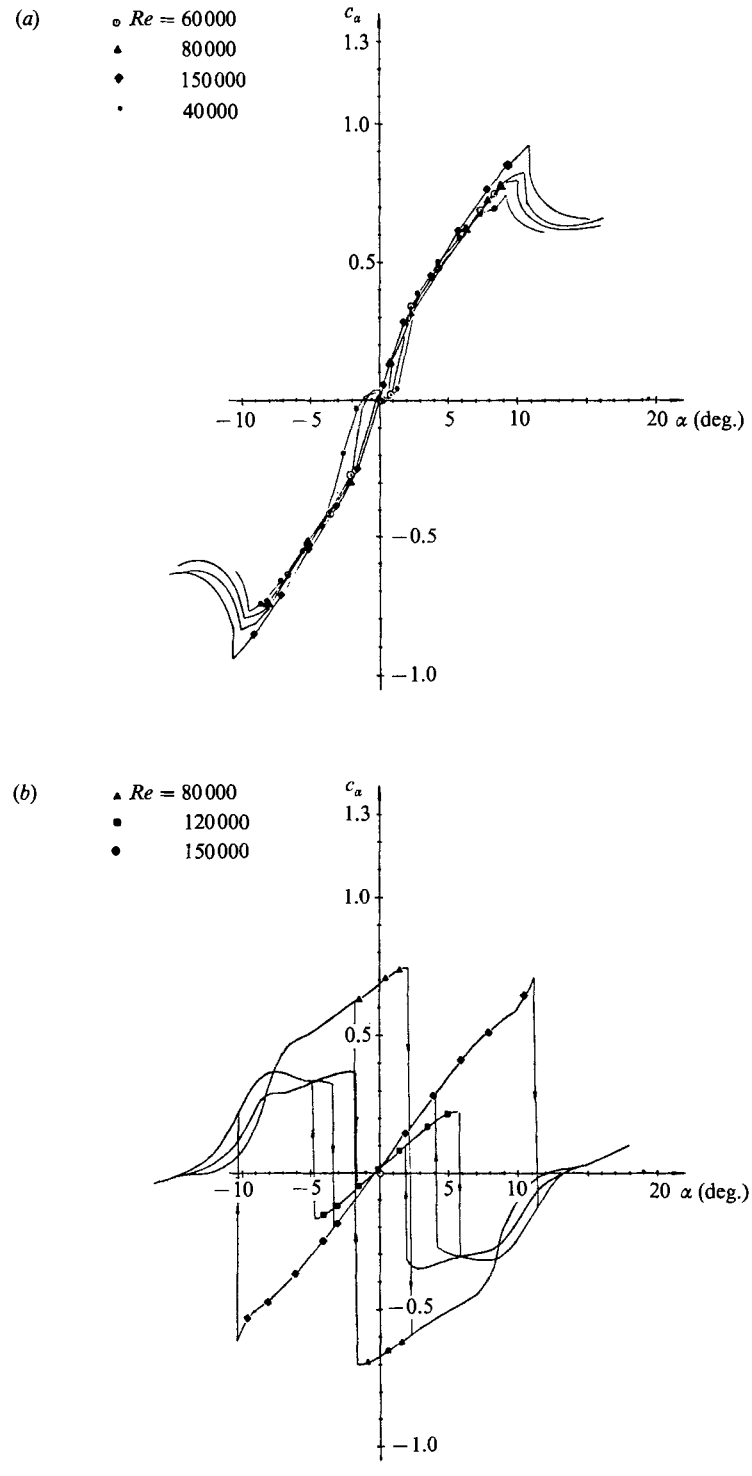

FIGURE 1. Section lift coefficient as a function of angle of attack for two symmetric NACA four-digit profiles at $Re = 40000$–150000 showing hysteresis and other lift anomalies: (*a*) NACA 0012, $d/c = 12\%$, $c = 120$ mm; (*b*) NACA 0033, $d/c = 33.3\%$, $c = 120$ mm. The data were generated at the laminar wind tunnel at the University of Stüttgart (Althaus 1980).

1.2. *Multiple steady states and symmetry breaking*

The possibility of having multiple solutions is not new to aerodynamicists familiar with lift hysteresis found in low-Re flows. In the framework of the present study, steady-state bifurcation can be brought out quite readily for thin obstacles in the domain $Re^{\frac{1}{16}}\tau = O(1)$; examples of the solution multiplicity have been given earlier for symmetric, thin airfoils (Cheng & Smith 1982). The simplicity gained through the theory for thin obstacles allows one to examine the possibility of symmetry breaking in an otherwise symmetrical flow, and to probe the bifurcating domain in the more general, asymmetrical cases. Open-wake solutions for airfoils based on this approach, including an example of symmetry breaking, were presented in several conference proceedings (Cheng 1984, 1985; Cheng & Lee 1985). The present paper focuses on the analysis of body-scale flows with closed wake which, together with the open-wake solutions, provide a more comprehensive description of the admissible steady-state, body-scale flows. Part of the results are discussed in Cheng (1986). To make the exposition more comprehensive, the open-wake analysis will be summarized and some of its more pertinent applications are also included for comparison.

1.3. *Forms of eddy/wake closure*

As indicated, Smith's (1985) formulation entails a cusp-shaped closure for the large eddy. There was a corresponding problem with a thin airfoil concerning the choice between a round (parabolic) end and a cuspidal end for the closure of a finite wake; but it follows from the drag analysis in Cheng & Smith (1982) that the round-end closure cannot provide a self-consistent, steady-state description. Cheng (1984) noted also that unless the stipulated scales for the flow velocity in the wake/eddy interior are changed, a closed wake with a round end would give rise to an extremely high-speed, re-entrant jet, leading to an unbalanced force on the closed wake itself. This leaves the cuspidal closure as the remaining viable choice for the *steady* body-scale flow, although a complete structure of the wake interior is lacking. This view receives support from the numerical findings of Rothmayer & Davis (1985) based on an interacting boundary-layer equation system; their results suggest that the re-entrant jet may not be present in a finite eddy. Even if the re-entrant jet were present, their results tend to suggest that such a jet will have no significant impact on the qualitative features described by the closed-wake model of Cheng & Smith (1982) and Cheng (1984). (Whether a time-dependent wake featuring a re-entrant jet can reach a steady state in this case remains an unsettled issue.) The arguments in favour of a stagnant wake/eddy and their cusp-end closure are maintained in this study; they may be considered as working hypotheses justified by their consistency with the steady-state model. The cusp-end closure appears to be in line with Smith's (1985) choice for his large-eddy model, even though the possibility for a large eddy with a unit-order aspect ratio will not be considered in the present study.

1.4. *Realizability*

The realizability of the steady-state, laminar-breakaway model is most evident perhaps from flow visualization experiments in the $Re = 10^3$–10^4 range, corresponding to the flight regime of insects, small birds, and indoor flying models. Figure 2 reproduces photo-records of streamlines about an airfoil made by H. Werlé (1974) in a flow visualization study in a water channel. The photographs, reproduced clearly in Van Dykes (1982), give streamline patterns at $Re \approx 7000$ for three attack angles. Their distinct streamline patterns lend strong support to the realizability as

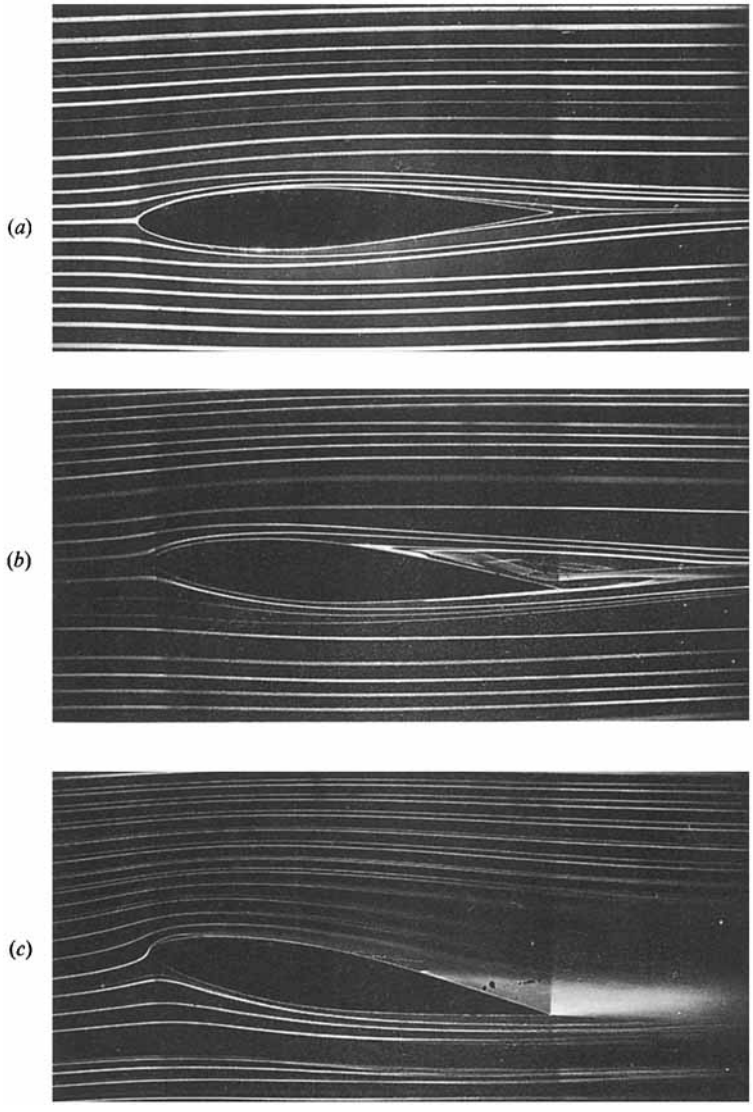

FIGURE 2. Photo records of streamlines about a NACA 64A015 section at $Re \approx 7000$ at three different attack angles reproduced from Werlé (1974). Note wake shape in (*b*) and the leading-edge eddy in (*c*).

well as the stability of the steady-state, laminar description for small and moderate incidences in this Re-range. The wake structure in the middle photograph indicates a rather weak backflow, and the convergence of the upper and lower shear layers therein also indicates the possibility of a *cuspidal* wake closure.

1.5. *The marginal separation*

An important application of the triple-deck theory to laminar separation is the analysis for a marginal situation in which a minute separation bubble occurs well within the boundary layer, and to which the global breakaway description considered here is not relevant. The problem, termed 'marginal separation', has been accorded much significance with respect to the instability and turbulence transition in high

subcritical as well as supercritical aerodynamic flows (Schmitz 1942; Tani 1964; Gaster 1967; Mueller 1979, 1985; Carmichael 1981; Lissaman 1983); it is also believed to underline the practical success of high-lift airfoil designs (Liebeck 1973; Eppler 1978). The triple-deck analyses of the marginal separation (Ruban & Sychev 1979; Cebeci, Stewartson & Williams 1980; Stewartson, Smith & Kaup 1982) and the subsequent instability studies (Elliot & Smith 1987) address their application to the onset problem of leading-edge stall. The inviscid–viscous interaction in this case does not involve a major alteration of the outer flow, and hence is strictly a local interaction problem. To distinguish them from the marginal separation just mentioned, the flows to be studied below (including both open and closed wakes) will be referred to either as *laminar breakaway* or as *massive laminar separation*. We point out in passing that sizable laminar separation bubbles are commonly observed on airfoils in the high subcritical and critical Re-range (Mueller 1979, 1985), which are far beyond the stage of a marginal separation, while features associated with wake and shear-layer instability are prominent.

2. Assumptions and working hypotheses

In the following, we state the several assumptions and types of flow models considered, which define the logical limitations of our study. Tentative working hypothesis such as those concerning the wake/eddy model, as well as several requirements resulting from the model's limitations and hypotheses, will be examined below.

We seek *steady-state* solutions to the problem of laminar breakaway in a slightly viscous, planar, incompressible body-scale flow. A triple-deck structure enclosing the separation point (Sychev 1972; Smith 1977) is assumed; together with the eddy/wake model, we stipulate that the body-scale flow so determined is consistent with the Navier–Stokes equations and non-slip wall conditions.

2.1. *Stagnant-wake/eddy models*

As noted earlier, photo records from flow visualization studies in many cases (Werlé 1974; Van Dyke 1982) as well as numerical findings of Rothmayer & Davis (1985) suggest a weak recirculating current interior to a laminar bubble or wake; therefore, a uniform eddy pressure will be postulated as a leading-order description of the body-scale flow. In the case of an open wake, this model is consistent with Kirchhoff's (1869) free-streamline theory (see Wu 1972) in which the wake pressure is taken to be that in the free stream p_∞, as was adopted in Sychev's (1972) original work.

For both the closed wake (in which the free shear layers reattach themselves behind the wing) and the laminar eddy/bubble (in which the free shear layer reattaches to the airfoil surface), their closure geometry will be assumed to be of a cusp shape (on the body scale) as indicated earlier; more specifically, it is $y \propto (l-x)^{\frac{3}{2}}$ where $x = l$ is the reattachment location. This appears to be consistent at least with the available photo records on the reattachment at $Re = 10^2 - 10^3$ (Werlé 1974), and is not unfamiliar in the classical cavity-flow theory (see Southwell & Vaisey 1946; Lighthill 1949; Wu 1972). The crucial distinction between cavity-flow theory and the present analysis lies, however, in the separation criterion applied at the breakaway location which was either taken to be the Brillouin–Villat point (see §2.2 below), or simply disregarded. The criterion used in the present study is based on the triple-deck theory for the breakaway, which leads to significant differences from cavity-

flow analyses for flows about thin obstacles. Additional remarks clarifying the triple-deck's role in the subsequent and related analyses are given below.

2.2. *Triple-deck theory applied to thin obstacles*

2.2.1. *Sychev's breakaway criterion*

Most fundamental among Sychev's (1972) results is the breakaway criterion on the pressure/velocity gradient of the body-scale flow, deduced from the solution to the reduced triple-deck problem. The argument leading to Sychev's criterion may begin with the recognition that, in approaching the breakaway location $x = s$ from upstream, the surface pressure of the body-scale flow must behave as

$$p - p_c \sim -k(s-x)^{\frac{1}{2}}, \tag{2.1}$$

where the constant of proportionality k is positive, and p_c is the cavity/eddy pressure downstream of $x = s$. In above, x and s are normalized by the body scale c, and p and p_c are normalized by twice the dynamic pressure based on the uniform flow speed directly over the eddy, i.e. ρu_c^2. The above behaviour follows from a consideration of the complex velocity of the body-scale flow near the juncture $x = s$ over a smooth boundary, where a Neumann condition at $x < s$ (for an impermeable surface) changes over to a Dirichlet condition at $x > s$ (over the eddy), which allows

$$p - p_c \sim -k(s-x)^{n+\frac{1}{2}}$$

for an arbitrary integer n. But a negative n would yield an unbounded pressure, whereas a positive n gives a zero pressure gradient for which the boundary layer will not separate. This leaves $n = 0$, thus (2.1), as the only choice. Note that the pressure gradient (on the body scale) is infinite as $x \to s$, according to (2.1), which is needed to provoke separation and breakaway in the triple deck. According to the triple-deck theory (e.g. Stewartson 1974), the variables $(p - p_c)$ and $(s - x)$ are small like ϵ^2 and ϵ^3, respectively, where

$$\epsilon \equiv Re^{-\frac{1}{8}} = \left(\frac{\mu}{\rho u_c c}\right)^{\frac{1}{8}}.$$

Therefore, the constant k of (2.1) must be small like $\epsilon^{\frac{1}{2}}$. In Sychev's analysis, k was expressed as a product of $\epsilon^{\frac{1}{2}}$ and a fractional power of unit-order quantity λ, which is the wall shear at $x = s$ immediately upstream of the triple-deck normalized by $\mu u_c / \epsilon^4 c$. More precisely, it is

$$k = \beta \lambda^{\frac{9}{8}} \epsilon^{\frac{1}{2}}, \tag{2.2}$$

where β is a unit-order constant determined from the theory (by matching the triple-deck solution with the square-root pressure/velocity behaviour of the body-scale flow (2.1)). Expressed more explicitly, Sychev's laminar breakaway criterion (2.1) takes the form

$$p - p_c \sim -\beta \lambda^{\frac{9}{8}} \epsilon^{\frac{1}{2}} (s-x)^{\frac{1}{2}}. \tag{2.3}$$

Smith (1977) gave $\beta \approx 0.44$ after solving numerically the reduced triple-deck problem; slightly lower values were obtained subsequently by Korolev (1980) and Van Dommelen & Shen (1983), with $\beta = 0.42$ and 0.41, respectively.

2.2.2. *Distribution between blunt and thin obstacles*

Since k, or the coefficient on the right-hand side of (2.3), vanishes in the limit $\epsilon \to 0$, the breakaway criterion could be identified with the location of a vanishing surface pressure gradient, or of the maximum surface speed (of the inviscid body-scale flow)

unless the obstacle is thin with its thickness vanishing also with ϵ. To a first approximation, the breakaway location $x = s$ in Sychev and Smith's analyses for a circular cylinder is therefore the same as the Brillouin–Villat point in the classical cavitating-flow theory (see Wu 1972). This location can of course be determined from the inviscid body-scale flow with the criterion $\mathrm{d}p/\mathrm{d}x = 0$, and does not depend on viscosity or Reynolds number.

The breakaway criterion (2.3) and the triple-deck structure (centred at $x = s$) are applicable also to airfoil-like thin obstacles, for which, however, the breakaway location cannot be generally identified with the zero-pressure gradient – the Brillouin–Villat point – as in Sychev and Smith's examples. In this case, the leading-order breakaway location ($x = s$) and its existence will depend, in accordance with (2.3), on viscosity through the ratio of an obstacle thickness ratio τ to $\epsilon^{\frac{1}{2}}$, called the rescaled thickness ratio

$$\tilde{\tau} \equiv \frac{\tau}{\epsilon^{\frac{1}{2}}} = Re^{\frac{1}{16}}\tau. \tag{2.4}$$

This parameter follows readily from (2.3), after one introduces the thickness ratio τ to gauge the pressure perturbation $(p - p_c)$ on the thin obstacle, as will be made more apparent later. To determine the breakaway location and the leading-order body-scale flow in this case, the criterion (2.3) must be used along with other boundary conditions. Obviously, the thickness ratio τ in (2.4) can be replaced by either an attack angle α or the airfoil camber σ to give a rescaled attack angle $\tilde{\alpha}$ or rescaled camber $\tilde{\sigma}$, respectively.

The range $\tilde{\tau} = O(1)$ pertaining to airfoils of thickness $\tau = O(\epsilon^{\frac{1}{2}}) \ll 1$ is the principal domain of the present study. As it turns out, the transition from a high $\tilde{\tau}$, corresponding to a blunt body, to $\tilde{\tau} = 0$ corresponding to an aligned flat-plate flow is not straightforward. Apart from a departure involving a trend reversal in the movement of the breakaway location as the thickness τ reduces, occurring in a range $\epsilon^{\frac{1}{2}} \ll \tilde{\tau} \ll 1$ (Brodetsky 1923; Cheng & Smith 1982), a great deal happens in the unit-order $\tilde{\tau}$-domain (Cheng & Smith 1982; Cheng 1984). A feature representing a significant departure from Sychev's original theory is the breakdown of the Kirchhoff open wake for $\tilde{\tau}$ falling below a certain critical value (for each family of affinely similar shapes), below which other steady-state models with wake closure must be considered. A more significant aspect is perhaps the multitude of steady states brought out quite readily by the analysis for the unit-order $\tilde{\tau}$ range. The solution bifurcation/branching should not be too surprising for $\tau = O(\epsilon^{\frac{1}{2}})$, since the rescaled pressure is not generally a simple function of s in this domain, i.e. (2.3) is a nonlinear equation for the unknown breakaway location s.

The cusp-shaped closure for the reattachment also implies a square-root pressure behaviour in the body-scale flow similar to (2.3), except that it applies at immediately downstream of the reattachment location $x = l$, with the algebraic sign in (2.3) changed to correspond to a favourable pressure gradient. The constant corresponding to β in (2.3) is generally unknown for the reattachment; its determination would require in some cases the solution of a multi-structure problem similar perhaps to that in Daniel (1979) study which treats a special supersonic outer flow. It turns out that, for a certain class of simple shapes involving a closed wake/eddy to be considered below, *a priori* knowledge of this constant and the flow detail at reattachment are not required for a complete determination of the steady body-scale solution, as will be seen in §3 below.

One may observe, in passing, that a parameter similar to the scaled attack angle

$$\tilde{\alpha} \equiv \epsilon^{-\frac{1}{2}}\alpha \tag{2.5}$$

mentioned above has appeared in the trailing-edge stall problem (Brown & Stewartson 1970; Melnik & Chow 1975); this is not too surprising since the triple deck around the flat-plate trailing edge considered is surrounded by a body-scale flow which is required to behave near the trailing edge in accordance with (2.3). But the constant β therein differs slightly owing to the mixed, asymmetric inner boundary condition for the lower deck, unlike the impermeable inner conditions assumed for the entire lower deck in Sychev's model adopted here. Brown & Stewartson (1970) and Melnik & Chow (1975) identified a critical scaled attack angle $\tilde{\alpha}_{\rm cr}$ with the vanishing of wall shear at the trailing edge, whereas Smith's (1983) analysis suggests that the point of vanishing wall shear can occur upstream of the trailing edge inside the triple deck at $\tilde{\alpha} > \tilde{\alpha}_{\rm cr}$. Whether a limiting solution from the trailing-edge stall study is consistent with the global structures analysed below is uncertain at present. The single-surface airfoil with shock-free entry considered in §5.2 and figure 14(*a*, *b*) will show that a range of $\tilde{\alpha}$ does exist, where the attached boundary-layer assumption stipulated in the three cited works can be satisfied on a global scale, and the consistency question may be examined in this case. We shall now examine the reduced boundary-value problem of the body-scale flow for several types of wakes and eddies, and describe briefly their solution procedures.

3. The boundary-value problem for the body-scale flow

3.1. *The linearized outer problem*

The consideration of τ, α or σ in the order-$\epsilon^{\frac{1}{3}}$ range permits linearization of the body-scale flow as in the classical thin-airfoil theory, subject to a relative error of order-ϵ. The Cartesian coordinates (x, y) are used and normalized by c, with the x-axis taken to be in the free-stream direction and its origin at the leading edge. The streamwise and transverse perturbation-velocity components are u and v, both normalized by τU_∞. The obstacle will be referred to either as an airfoil or as a wing. The wing surface ordinates are expressed as

$$y^{\pm} = \tau f^{\pm}(x), \quad 0 < x < 1, \tag{3.1}$$

where the superscripts + and − refer to the upper and lower surface, respectively. An angle of attack or camber is allowed inasmuch as symmetry in the airfoil geometry is not required, i.e. $f^{+}(x) \neq -f^{-}(x)$ generally. As is common in classical airfoil theory, τ can be replaced by α or σ as controlling parameter, if the latter effect prevails.

3.2. *Linearized forms for pressure, open wake, closed wake and eddies*

In linearized forms, the impermeable wing boundary condition reduces to $v^{\pm} = \mathrm{d}f^{\pm}/\mathrm{d}x$ on the unseparated part of the wing surface, and over an eddy/wake the boundary condition is $u = u_{\rm c}$, a constant. These boundary conditions may be analytically transferred to the corresponding segments on the upper and lower sides of the x-axis, according to the standard practice of thin-airfoil theory (Glauert 1926; Ashley & Landahl 1965). We define the perturbation pressure to be the difference from the free-stream pressure $(p^{*}-p^{*}_{\infty})$, i.e. $\rho U^{2}_{\infty}(p-p_{\infty})$. Thus, after linearization, $(p-p_{\rm c})$ in (2.3) is linearly related to $(u-u_{\rm c})$ as

$$p-p_{\rm c} = -\tau(u-u_{\rm c}), \tag{3.2}$$

where $u_{\rm c}$ over the eddy is related to the normalized cavity/eddy pressure $p_{\rm c}$ as

$$u_{\rm c} = -\frac{p_{\rm c}-p_{\infty}}{\tau}. \tag{3.3}$$

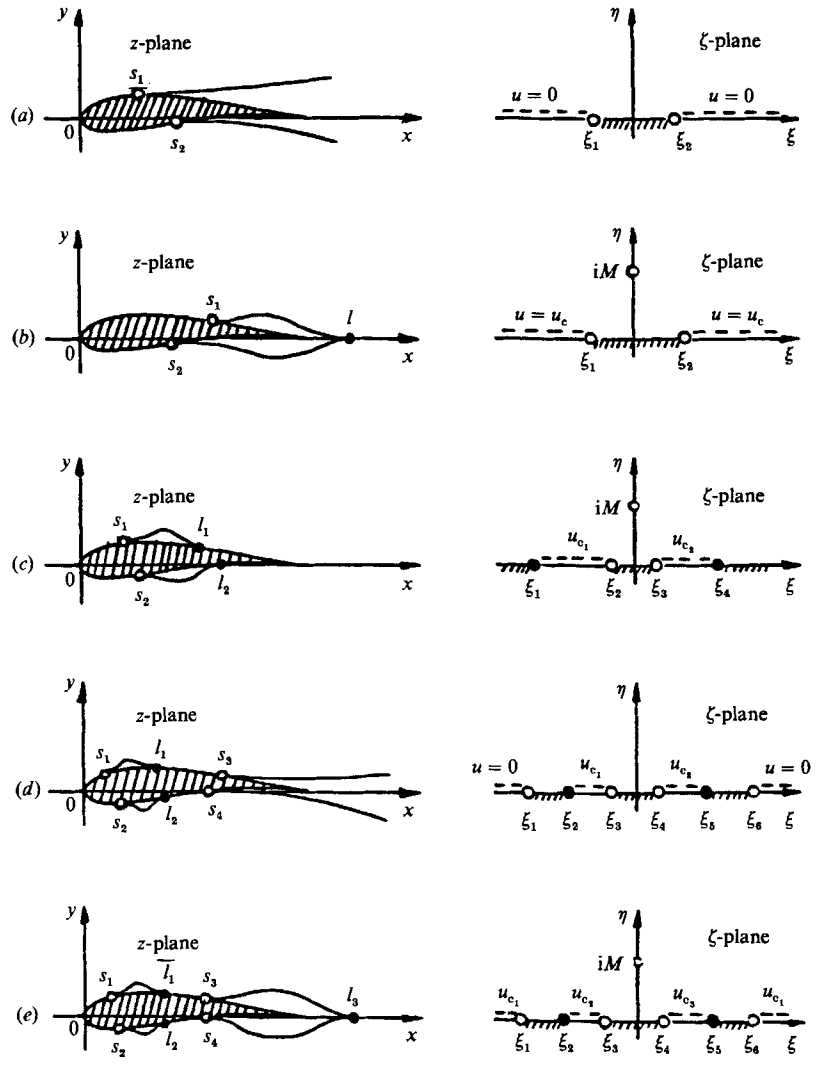

FIGURE 3. Classification of wake and eddy configurations in the body-scale flows, definition of the breakaway and reattachment locations, and the mapping from z- to ζ-plane.

There will be as many values of u_c as breakaway locations allowed in the global flow model. It is not known *a priori* whether, in the limit in which the wake length tends to infinity, the closed-wake model considered may yield $p_c \to p_\infty$ or $u_c \to 0$ to agree with Kirchoff's value for an open wake. One essential result brought out by the present study is that u_c indeed vanishes as the wake length becomes unbounded.

For a uniform free stream, the global problem is irrotational and reduces to finding a complex velocity $dw/dz = u - iv$ for the mixed boundary-value problem described above, which must also meet the requirements for the breakaway and reattachment behaviour. Figure 3(*a–e*) illustrates the boundaries and solution domains for five types of wakes and eddies in the plane $z = x + iy$ and also in a transformed ζ-plane where the asymmetrical body-scale flow can be more effectively solved as a half-plane problem. Global flow models allowing similar but more intricate wake/eddy structures can be constructed, requiring more complex analytical details, however.

3.3. *Application of the laminar breakaway criterion*

The linearization of the equations governing the body-scale flow not only provide a simpler boundary-value problem to be solved, but greatly reduce the work of evaluating the wall shear parameter λ in (2.3), which would otherwise require integrating the non-self-similar boundary-layer equation up to the breakaway point. Since the velocity field about an airfoil on the body scale is only slightly perturbed from a uniform flow, the flow speed at the boundary-layer outer edge can be taken to be U_∞, subject to a relative error of order τ. This linearization procedure breaks down however in the vicinity of the leading edge (Lighthill 1951; Van Dyke 1975); we assume that the (relative) error in the boundary-layer calculation at $x \neq 0$ resulting from this breakdown is no worse than that in the thin-airfoil theory. Taking the leading-edge radius to be of order τ^2, this region of non-uniformity is $x = O(\tau^2)$, being comparable with ϵ in the parameter domain of interest. In the meantime, a consistent linearization of body-scale flow together with the triple-deck breakaway criterion requires s to be sufficiently far removed from the leading edge as well as from the trailing edge. This consideration would require the breakaway location to fall into

$$\epsilon^3 \ll s \ll 1-\epsilon^3,$$

recalling that ϵ^3 is the streamwise triple-deck lengthscale. Taking the leading-edge non-uniformity also into account, the range of s where the linearized breakaway condition (2.3) can be applied without inconsistency should then be

$$\epsilon \ll s \ll 1-\epsilon^3. \tag{3.4}$$

With this provision, the attached boundary layer can be determined from the Blasius self-similar solution, up to $x = s$, the first breakaway on each side of the airfoil. The value of λ in (2.3) may thus be taken to be the Blasius value $\lambda = 0.332$. Therefore, at the first breakaway location, criterion (2.3) will be simplified to

$$\lim_{x \to s} \frac{u-u_c}{(s-x)^{\frac{1}{2}}} = \frac{\beta(0.332)^{\frac{9}{8}}}{\tilde{\tau} s^{\frac{9}{16}}}, \tag{3.5}$$

where u is the real part of $\mathrm{d}w/\mathrm{d}z$ mentioned earlier. For a body-scale flow involving more than one breakaway location on the same side of the airfoil, as in figures 3(*d*) and 3(*e*), the constant λ must be re-evaluated (at s_3 and s_4 in figures 3*d*, 3*e*) for the boundary layer downstream of a reattachment point (l_1 or l_2 in figures 3*d*, 3*e*).

3.4. *The requirement on the far field and also on wake and eddy closure*

The enforcement of the appropriate solution behaviour at $|z| \to \infty$ and at the wake/eddy closure point $z = l$, together with the criterion at each breakaway location, is essential to the determination of the steady-state solution for type (*a*), (*b*) and (*c*) flows of figure 3, and to the final reduction to a single-parameter solution family for type (*e*) and (*d*). For the far field with an open wake, the behaviour

$$u - \mathrm{i}v \sim \frac{-\mathrm{i}k_\infty}{z^{\frac{1}{2}}} \tag{3.6}$$

is imposed, where k_∞ is required to be a real and positive constant to be expressible in terms of the wing geometry and s_1 and s_2, etc. (cf. figure 3); this requirement assures a pair of Kirchhoff streamlines in the far wake. The vanishing of k_∞ signifies

the breakdown condition for the Kirchhoff-wake model and has been referred to as 'wake cut off' (Cheng & Smith 1982). For a closed wake or the case without a wake, a doublet behaviour in the far field is appropriate:

$$u-\mathrm{i}v \sim \frac{\mathrm{i}}{2\pi}\frac{\Gamma}{z}+O\left(\frac{1}{z^2}\right), \tag{3.7}$$

where the constant Γ is identified with the circulation and must be real.

The eddy-closure model discussed earlier requires the behaviour near the closure point to be

$$u-\mathrm{i}v \sim \text{const.}+m(z-l)^{\frac{1}{2}}, \tag{3.8}$$

where m is a constant to be determined by the final solution and must be positive and real to assure a cuspidal closure.

3.5. *Determination of the breakaway and reattachment location: solution strategy*

We adopt Carleman's (1922) technique to solve each of the half ζ-plane problems (cf. figure 3), which permits an explicit expression for $\mathrm{d}w/\mathrm{d}\zeta \equiv \mathscr{U}-\mathrm{i}\mathscr{V}$, where $\mathscr{U}$ and $-\mathscr{V}$ are the real and imaginary parts of $\mathrm{d}w/\mathrm{d}\zeta$, in terms of the real and imaginary parts of $\mathrm{d}w/\mathrm{d}z$ alternately prescribed over the real ζ-axis (Cheng & Rott 1954). The behaviour at the breakaway and reattachment locations according to (3.5) and (3.8) requires a square-root singularity at each of the junctions $\zeta = \xi_1, \xi_2, \xi_3, \ldots$ etc. on the real ζ-axis, corresponding to each of the $x = s_1, s_2, \ldots, l_1, l_2, \ldots$ etc. on the upper and lower segments on the real z-axis. Let

$$H(\zeta) \equiv [(\zeta-\xi_1)(\zeta-\xi_2)(\zeta-\xi_3)\ldots(\zeta-\xi_N)]^{\frac{1}{2}}Q(\zeta), \tag{3.9}$$

where $Q(\zeta)$ is a quotient of polynomials which may be needed to suit the desired behaviour of $\mathrm{d}w/\mathrm{d}\zeta$ at some locations in the ζ-plane other than the vicinities of ξ_j. The expression sought is

$$\mathscr{U}-\mathrm{i}\mathscr{V} = -\frac{H(\zeta)}{\pi}\int_{\xi_1}^{\xi_N}\frac{q(\xi')\,\mathrm{d}\xi'}{\zeta-\xi'}, \tag{3.10}$$

where the source-like function $q(\xi')$ is

$$q(\xi) = \frac{\mathscr{V}(\xi,0)}{H(\xi)}, \quad \mathrm{i}\frac{\mathscr{U}(\xi,0)}{H(\xi)}$$

over the segment of ξ where $H(\xi)$ is real and imaginary, respectively. It is understood that the boundary values for $\mathscr{V}$ and $\mathscr{U}$, as well as $H(\xi)$, are taken along the upper side of the real axis, and that the distribution $q(\xi)$ is real. Application of (3.10) to the requirement on $\mathrm{d}w/\mathrm{d}z$ at $|z| \to \infty$ and to the breakaway criterion at each of $s_1, s_2, \ldots$ provide the needed equations for determining $s_1, s_2, \ldots, l_1, l_2, \ldots$, for type (*a*), (*b*) and (*c*) flows. We point out in passing that, instead of solving for $\mathrm{d}w/\mathrm{d}\zeta = \mathscr{U}-\mathrm{i}\mathscr{V}$, we can solve for $\mathrm{d}w/\mathrm{d}z = u-\mathrm{i}v$ also in the half-ζ-plane, since u and v remain conjugate in the transformed plane.

Velocity field for type (a) wakes

For a type (*a*) open wake of figure 3, with the mapping

$$\zeta = z^{\frac{1}{2}}, \tag{3.11}$$

there are two junctures $\zeta = \xi_1 = -s_2^{\frac{1}{2}}$ and $\zeta = \xi_2 = s_1^{\frac{1}{2}}$ on the real axis. Over the segments $\xi < \xi_1$ and $\xi > \xi_2$ corresponding to the Kirchhoff streamlines, the real part

of $\mathrm{d}w/\mathrm{d}\zeta$ is zero; and over $\xi_1 < \xi < \xi_2$ corresponding to the part of the airfoil with attached boundary layer, the imaginary part of $\mathrm{d}w/\mathrm{d}\zeta$ is

$$\begin{aligned} \nu(\xi, 0) &= -2\xi v_0^-(\xi^2) \quad \text{at} \quad \xi_1 < \xi < 0 \\ &= -2\xi v_0^+(\xi^2) \quad \text{at} \quad 0 < \xi < \xi_2, \end{aligned}$$

where $v_0^{\pm}(x) = \mathrm{d}f^{\pm}/\mathrm{d}x$. The complex velocity $\mathrm{d}w/\mathrm{d}z$ satisfying the far-field behaviour (3.6) may then be written in this case as

$$\frac{\mathrm{d}w}{\mathrm{d}z} = \frac{-\mathrm{i}[(\zeta-\xi_1)(\zeta-\xi_2)]^{\frac{1}{2}}}{\pi\zeta} \int_{\xi_1}^{\xi_2} \frac{\xi' v_0((\xi'))\,\mathrm{d}\xi'}{[(\xi_2-\xi')(\xi'-\xi_1)]^{\frac{1}{2}}(\zeta-\xi')}, \tag{3.12}$$

with

$$\begin{aligned} v_0((\xi)) &= v_0^-(\xi^2) \quad \text{at} \quad \xi_1 < \xi < 0 \\ &= v_0^+(\xi^2) \quad \text{at} \quad 0 < \xi < \xi_2. \end{aligned} \tag{3.13}$$

The constant of proportionality k_∞ in (3.6) can be evaluated from

$$k_\infty = \frac{2}{\pi} \int_{\xi_1}^{\xi_2} \frac{\xi' v_0((\xi'))\,\mathrm{d}\xi'}{[(\xi'-\xi_1)(\xi_2-\xi')]^{\frac{1}{2}}}, \tag{3.14}$$

which is required to be positive for an open wake. Application of the breakaway condition (3.5) leads to two nonlinear equations for the determination of s_1 and s_2 for a given $\tilde{\tau}$ and $v_0^{\pm}(x)$:

$$\frac{\pi\sqrt{2\bar{\beta}}}{\tilde{\tau}} = \frac{(\xi_2-\xi_1)^{\frac{1}{2}}}{\xi_2^{\frac{3}{8}}} \int_{\xi_1}^{\xi_2} \frac{\xi' v_0((\xi')) - \xi_2 v_0((\xi_2))}{(\xi'-\xi_1)^{\frac{1}{2}}(\xi_2-\xi')^{\frac{3}{2}}}\,\mathrm{d}\xi', \tag{3.15}$$

$$\frac{\pi\sqrt{2\bar{\beta}}}{\tilde{\tau}} = \frac{(\xi_2-\xi_1)^{\frac{1}{2}}}{|\xi_1|^{\frac{3}{8}}} \int_{\xi_1}^{\xi_2} \frac{\xi' v_0((\xi')) - \xi_1 v_0((\xi_1))}{(\xi_2-\xi')^{\frac{1}{2}}(\xi'-\xi_1)^{\frac{3}{2}}}\,\mathrm{d}\xi', \tag{3.16}$$

where $\bar{\beta} = (0.332)^{\frac{9}{8}}\beta$.

Velocity field for type (b) wakes

For a type (*b*) closed wake of figure 3, the reduced half-plane problem may again be made to allow two juncture points on the real axis. The mapping in this case, adopted from Wu's (1972) analysis of cavitating thin hydrofoils, is

$$\zeta = \mathrm{i}M \frac{z^{\frac{1}{2}}}{(z-l)^{\frac{1}{2}}}, \tag{3.17}$$

where M is a real and positive constant. It maps the closure point $z = l$ to $|\zeta| \to \infty$, and $|z| \to \infty$ to a point on the imaginary axis $\zeta = \mathrm{i}M$. The breakaway points on the lower and upper surfaces s_2 and s_1 are mapped to

$$\xi_1 = M \frac{s_2^{\frac{1}{2}}}{(l-s_2)^{\frac{1}{2}}}, \quad \xi_2 = -M \frac{s_1^{\frac{1}{2}}}{(l-s_1)^{\frac{1}{2}}}$$

respectively. For this problem, it proves expedient to solve directly for the conjugate pair (u, v) in the ζ-plane. Thus over $\xi_1 < \xi < \xi_2$, $v = v_0((\xi))$, and $u = u_c$ elsewhere on the real axis. In this case, we choose $H(\zeta)$ in (3.9) to be

$$H(\zeta) = \mathrm{i}[(\zeta-\xi_1)(\zeta-\xi_2)]^{\frac{1}{2}} \frac{\zeta^2+M^2}{\zeta}. \tag{3.18}$$

The function $u-iv$ may now be expressed as

$$\frac{dw}{dz}=\frac{-i(\zeta^2+M^2)}{\pi\zeta}[(\zeta-\xi_1)(\zeta-\xi_2)]^{\frac{1}{2}}\left\{u_c\int_{-\infty}^{\xi_1}\frac{\xi'\,d\xi'}{[(\xi_1-\xi')(\xi_2-\xi')]^{\frac{1}{2}}(\xi'^2+M^2)(\zeta-\xi')}\right.$$
$$+\int_{\xi_1}^{\xi_2}\frac{\xi' v_0((\xi'))\,d\xi'}{[(\xi'-\xi_1)(\xi_2-\xi')]^{\frac{1}{2}}(\xi'^2+M^2)(\zeta-\xi')}$$
$$\left.-u_c\int_{\xi_2}^{\infty}\frac{\xi'\,d\xi'}{[(\xi'-\xi_1)(\xi'-\xi_2)]^{\frac{1}{2}}(\xi'^2+M^2)(\zeta-\xi')}\right\},$$

where the first and last integrals can be evaluated analytically so that

$$\frac{dw}{dz}=u_c+\frac{-iu_c[(\zeta-\xi_1)(\zeta-\xi_2)]^{\frac{1}{2}}}{\zeta}\frac{\zeta\sin\Theta+M\cos\Theta}{[(M^2+\xi_1^2)(M^2+\xi_2^2)]^{\frac{1}{4}}}$$
$$-\frac{i(\zeta^2+M^2)}{\pi\zeta}[(\zeta-\xi_1)(\zeta-\xi_2)]^{\frac{1}{2}}\int_{\xi_1}^{\xi_2}\frac{\xi' v_0((\xi'))\,d\xi'}{[(\xi'-\xi_1)(\xi_2-\xi')]^{\frac{1}{2}}(\xi'^2+M^2)(\zeta-\xi')},\quad(3.19)$$

with $\Theta=\frac{1}{2}(\theta_1+\theta_2)$, $\theta_1=\pi+\tan^{-1}(M/\xi_1)$, and $\theta_2=\tan^{-1}(M/\xi_2)$.

Application of the breakaway criterion at $z=s_1$ and $z=s_2$ (transformed to $\zeta=\xi_1$ and ξ_2) together with the solution behaviour required for $\zeta\to iM$ and $|\zeta|\to\infty$ suffice for the determination of the four quantities s_1, s_2, u_c and l *for a* prescribed $f^{\pm}(x)$ for a specified rescaled thickness ratio $\tilde{\tau}$.

Velocity field for type (c) flow

The wakeless type (*c*) with a mid-wing eddy may be treated like type (*b*), with the same transformation (3.17) except that the closure-point location $x=l$ therein is replaced by the trailing-edge position $x=1$:

$$\zeta=iM\frac{z^{\frac{1}{2}}}{(z-1)^{\frac{1}{2}}}.\quad(3.20)$$

The four unknown locations s_1, s_2, l_1 and l_2 (see figure 3*c*) and two eddy pressures (or u_{c_1} and u_{c_2}) can be determined by requirements corresponding to the two breakaway conditions at $x=s_1, s_2$, the non-source behaviour in the far field at $|z|\to\infty$, with cuspidal reattachment at $x=l_1, l_2$ and the Kutta condition at $x=1$. Examples of type (*c*) have been studied in Cheng (1984) for symmetrical flows about symmetric airfoils.

Type (d) open-wake flow: indeterminacy

The complex-velocity field of type (*d*) flow in figure 3, which allows a second breakaway on each side of the airfoil to form an open wake after reattachment, can be constructed in the upper half-plane of $\zeta=z^{\frac{1}{2}}$ in a manner similar to the type (*a*) flow, following Carleman's (1922) approach. In this case, the function $H(\zeta)$ of (3.9) will be taken as a product of six roots at $\xi_1=-s_4^{\frac{1}{2}}$, $\xi_2=-l^{\frac{1}{2}}$, $\xi_3=-s_2^{\frac{1}{2}}$, $\xi_4=s_1^{\frac{1}{2}}$, $\xi_5=l^{\frac{1}{2}}$ and $\xi_6=s_3^{\frac{1}{2}}$, corresponding to the breakaway and reattachment points. Over $\xi<\xi_1$ and $\xi>\xi_6$ on the real axis, $\mathscr{U}$ must vanish; over $\xi_2<\xi<\xi_3$, $\mathscr{U}=2\xi u_{c_1}$; over $\xi_4<\xi<\xi_5$, $\mathscr{U}=2\xi u_{c_2}$; over the remainder of the real axis, $\mathscr{V}=v_0((\xi^2))$ defined in (3.13). The six root locations and two eddy pressure or u_{c_1} and u_{c_2} are the eight unknown constants to be determined for prescribed affined ordinates $f^{\pm}(x)$ at a

specified $\tilde{\tau}$. But this construction gives a behaviour of $\mathrm{d}w/\mathrm{d}z$ in the physical far field ($|z| \to \infty$) of the form

$$\frac{\mathrm{d}w}{\mathrm{d}z} = \frac{1}{2\zeta}\frac{\mathrm{d}w}{\mathrm{d}\zeta} \sim A_\infty z^{\frac{1}{2}} + B_\infty + \frac{C_\infty}{z^{\frac{1}{2}}} + \ldots . \tag{3.21}$$

The Kirchhoff open wake so stipulated therefore requires (cf. (3.6)) that

$$A_\infty = B_\infty = 0 \tag{3.22}$$

and that C_∞ be negatively imaginary. These, together with the four breakaway criteria at $x = s_1, s_2, s_3$ and s_4 furnish six conditions for the determination of the eight unknowns noted above. Thus two degrees of freedom remain with this steady-state model. The system could be closed with a specification of either the eddy pressure, i.e. u_c, or the eddy length l for each mid-wing eddy/bubble.

One may argue that the indeterminacy of the global description may reflect the need for a reattachment criterion derived from a local inviscid–viscous interaction of the reattaching shear layer, wall boundary layer, and the recirculating eddy/bubble. This specific knowledge is lacking even for the relatively simple case involving a supersonic external flow (see Daniels 1979). An attractive approach to this indeterminacy is to study the global instability of this body-scale description, and to identify the stable or the least unstable configurations. However, this line of enquiry can at best provide an inequality among the flow parameters, and is therefore not helpful in the solution determination for the steady states.

Cheng & Lee (1985) considered a special version of the flow type which invoked an open wake with the breakaway and reattachment occurring only on one side of the airfoil. Apart from the indeterminacy note above, complication and uncertainty in analysing this type of flow model arises in the evaluation of the λ in (2.3) for the second breakaway, which is the normalized wall shear immediately upstream of the triple deck and has been taken to be 0.332 in (3.5). For the second breakaway downstream of a reattachment on the surface, the boundary layer can no longer be described by the Blasius solution even under the simplification for a nearly uniform, external flow. In the absence of an appropriate non-self-similar solution for the determination of λ at the second breakaway, Cheng & Lee (1985) proposed a value based on a plane half-jet solution (Lock 1951) with the jet origin set at the upstream reattachment point. Their stipulation is yet to be substantiated by a more thorough analysis of the reattachment process, unavailable to date.

Type (e) closed-wake flow

The velocity field of this type of body-scale flow (cf. figure 3*e*) can be studied in a manner similar to that for the closed-wake type (*b*), using the same mapping (3.17). The three unknowns, e.g. s_1, l_1 and u_{c_1}, associated with each eddy/bubble on the wing, by virtue of the stronger attenuation requirement in the fair field, (3.7), will not introduce indeterminacy as occurred for type (*d*) with an open wake. The complication and the uncertainty in evaluating λ at the second breakaway remain, however.

In view of the indeterminacy and uncertainty encountered in the analysis of type (*d*) and (*e*) flows, the examples of body-scale flows to be studied below will be limited to the simpler model types (*a*) and (*b*). As noted, examples of type (*c*) have been considered for symmetric cases; asymmetrical type (*c*) solutions have not been studied.

4. An example of open and closed wakes: a model Joukowski profile

Examples of symmetric airfoils were studied in Cheng & Smith (1982) to illustrate the Kirchhoff-wake breakdown and multiple solutions of the open and closed wakes. The bifurcating steady states which allow asymmetrical solutions with lift were investigated in Cheng (1984, 1985), and Cheng & Lee (1985). With the exception of symmetrical cases at zero lift, cited studies have been restricted to the open-wake type (*a*) flow. In the following, the asymmetric solutions with the type (*b*) closed wake will be added to the multiple solutions for the symmetric model Joukowski airfoil, making the analysis of the bifurcating states more complete.

4.1. *A model symmetric Joukowski airfoil*

The particular profile considered has a symmetric cross-section with a round leading edge and a sharp trailing edge:

$$y = \pm\tau x^{\frac{1}{2}}(1-x)(1+Cx)$$

for which a relatively simple solution form can be obtained for type (*a*) open-wake flow. The normalized upwash on the unseparated portions of the upper and lower wing surfaces, allowing an angle of attack, is

$$v_0^{\pm}(x) = \frac{\alpha}{\tau} \pm \frac{1}{2x^{\frac{1}{2}}}[1-3(1-C)x-5Cx^2].$$

The particular case to be analysed in detail is one with $C=-1$, that is

$$y = \frac{\alpha}{\tau} \pm \tau x^{\frac{1}{2}}(1-x)^2. \tag{4.1}$$

This profile has a leading-edge radius of $O(\tau^2)$ and a *cusp-ended* trailing edge at $x=1$, it may hence be regarded as a model of a Joukowski airfoil. The following will examine the multitude of these asymmetrical results for type (*a*) open wakes and study a broader class of asymmetrical flows including type (*b*) closed wakes.

4.2. *Stipulations to be verified: unseparated flow as an alternative*

Stipulated in the problem formulation is that the breakaway streamline corresponding to the free shear layer does not intersect the wing surface. This is not guaranteed however by the boundary condition $u = u_c$, over the separated streamline. Another stipulation implicit in the formulation for the global problem is that the boundary layer remains attached until reaching the neighbourhood of the breakaway point. Both of these assumptions should be verified *a posteriori*, if the solution obtained from the asymptotic theory is to represent a physically meaningful steady state for a specified τ or Re. One may recall that the asymptotic (triple-deck) theory underlying the present analysis holds for a finite $\tilde{\tau} \equiv Re^{\frac{1}{16}}\tau \neq 0$ in the limit $Re \to \infty$ or $\tau \to 0$. In this limit, the flow speed at the boundary-layer outer edge is $u^* = U_\infty$, and the boundary layer should not separate, at least upstream of the triple deck. Separation and breakdown of the boundary layer could nevertheless occur upstream of the triple-deck in the domain of $\tilde{\tau} = O(1)$ for some $\tau \neq 0$ which is not small enough to allow the approximation $u^* \approx U_\infty$ at the outer edge.

It is essential to observe that, for a family of affinely similar profiles at a fixed α/τ in (4.1), a fully attached laminar flow can exist for a sufficiently small thickness ratio τ. This is because the condition for separation in a two-dimensional boundary layer,

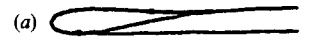

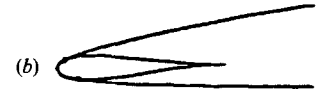

FIGURE 4 FIGURE 5 FIGURE 6

FIGURE 4. The breakaway streamlines from a model Joukowski airfoil for the reduced thickness $\tilde{\tau} \equiv Re^{\frac{1}{16}}\tau = 0.2$ at three angles of attack according to open-wake solutions on the central branch. (*a*) $\alpha/\tau = 0$, $C_L/\tau = 0$; (*b*) $\alpha/\tau = 0.25$, $C_L/\tau = -0.0538$; (*c*) $\alpha/\tau = 0.517$, $C_L/\tau = -0.2471$.

FIGURE 5. The breakaway streamlines from a model Joukowski airfoil for the reduced thickness $\tilde{\tau} = 0.2$ at three angles of attack according to open-wake solutions on the lower branch. (*a*) $\alpha/\tau = 0$, $C_L/\tau = -1.2755$; (*b*) $\alpha/\tau = 0.25$, $C_L/\tau = -0.8460$; (*c*) $\alpha/\tau = 0.48$, $C_L/\tau = -0.4081$.

FIGURE 6. The breakaway streamlines from a model Joukowski airfoil for the reduced thickness $\tilde{\tau} = 0.2$ at three angles of attack according to open-wake solutions on the upper branch. (*a*) $\alpha/\tau = 0$, $C_L/\tau = 1.2755$; (*b*) $\alpha/\tau = 0.075$, $C_L/\tau = 1.4014$; (*c*) $\alpha/\tau = 0.175$, $C_L/\tau = 1.5415$.

according to the normalized form of the boundary-layer equations and boundary conditions, is controlled by the pressure distribution in the outer flow, or more precisely by $(\partial p/\partial x)/\rho u_\infty^2 l^{-1}$, and hence by the thickness ratio τ. For $\tau \neq 0$, a maximum thickness ratio for an attached flow corresponding to the first appearance of a zero wall shear, or marginal separation, can be determined (for a fixed α/τ), independently of the Reynolds number Re or the scaled thickness ratio $\tilde{\tau}$. Hence, for a thickness ratio τ less than this value, a fully attached flow should be possible along with the other steady-state separated flows analysed below.

4.3. *Three solution branches for an open wake*

The model symmetric airfoil (4.1) has three solution branches for a type (*a*) open wake. One, to be called the central branch, gives a symmetrical flow pattern at zero incidence, and the other two, to be referred to as the upper and lower branches, yield (non-zero) lifts at zero incidence, providing an example of symmetry breaking. The breakaway locations on the upper and lower surfaces, s_1 and s_2 respectively, are determined as functions of $\tilde{\tau} \equiv Re^{\frac{1}{16}}\tau$ for several values of incidence to thickness ratio α/τ. For small and moderate α/τ, the two locations s_1 and s_2 in the central branch differ only slightly, giving a nearly symmetric flow pattern and hence little lift. In the

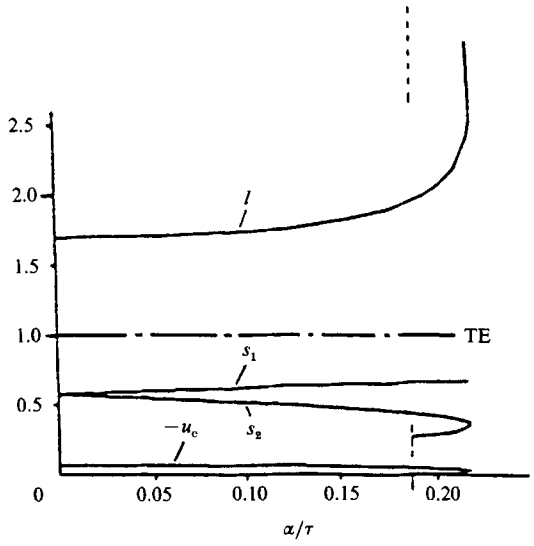

FIGURE 7. Breakaway locations (s_1 and s_2), closure locations (l), and the normalized eddy pressure ($-u_c$) over a model Joukowski airfoil of reduced thickness $\tilde{\tau} = 0.2$ as functions of incidence-to-thickness ratio according to a closed-wake solution.

other two branches, s_1 and s_2 are wide apart; the lower branch with $s_1 < s_2$ gives an appreciable negative lift. Note that the portion of attached flow is large on the lower side in this case. The upper branch with $s_1 > s_2$ has a positive lift. Numerical details for this open-wake case have been discussed in Cheng & Lee (1985), and will not be repeated here. To illustrate the departure from a fully attached flow, the streamlines representing the free-shear layer leaving the breakaway points are shown for $\tilde{\tau} = 0.20$ in figures 4–6 for each of the three solution branches at different values of α/τ. The result for the central branch at $\alpha = 0$ in figure 4(a) may be identified with the classical Kirchhoff streamlines. The corresponding lift characteristics, C_L *vs.* α, will be studied together with the closed-wake results later, in §4.5.

4.4. *Solutions with closed wakes*

Steady-state solutions of type (b) featuring a closed wake exist in a certain domain of $\tilde{\tau}$ and α/τ. The results presented in figures 7–12 illustrate the body-scale flows of this type about the model Joukowski airfoil (4.1) at incidence for three different reduced thicknesses, $\tilde{\tau} = 0.20$, 0.373 and 0.45.

4.4.1. *Breakaway locations, wake length and eddy pressure*

The basic information on the solutions for $\tilde{\tau} = 0.20$ is given in figure 7 where the upper and lower breakaway locations, s_1 and s_2, the closure location l, and the eddy pressure $-u_c$ are presented as functions of the incidence ratio α/τ. As the attack angle increases, s_1 and s_2 move downstream and upstream respectively, thus increasing the lift. Only the positive range of α/τ is shown; the corresponding results for the negative α/τ can be obtained by simply replacing α/τ with $-\alpha/\tau$ and interchanging s_1 and s_2 in the same plot. The range of α/τ for the closed-wake solution is seen to be rather limited in this case. Over the incidence range $0 < \alpha/\tau \leqslant 0.18$, the wake lengthens slightly with increasing incidence. Between $0.18 \leqslant \alpha/\tau \leqslant 0.22$, the closed-wake solutions have multiple values (bifurcate); while the lower branch of l continues to increase with α/τ for $\alpha/\tau > 0.18$, the upper branch of l decreases from

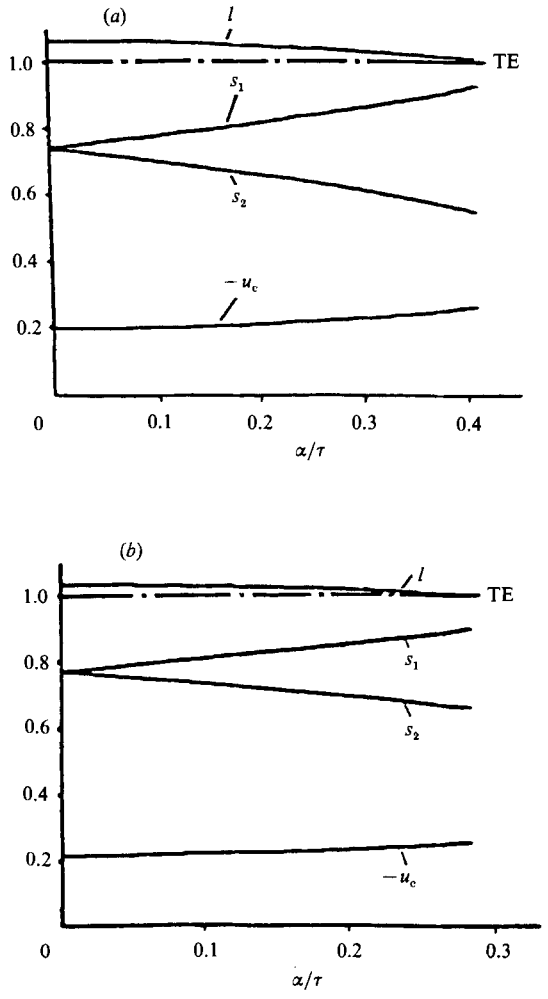

FIGURE 8. Breakaway and closure locations, and eddy pressure over a model Joukowski airfoil for two reduced thickness ratios, (*a*) $\tilde{\tau} = 0.373$, (*b*) $\tilde{\tau} = 0.45$ as functions of incidence-to-thickness ratio according to a closed-wake solution.

infinity (at $\alpha/\tau \approx 0.18$) as α/τ increases. Thus the branch with the higher l signifies a continuation of one of the type (*a*) open-wake solutions after the Kirchhoff wake breaks down. This will be more clearly brought out in the discussion of figure 11 on the lift. The value of $-u_c$ is seen to change very little with α/τ, indicating also that the eddy pressure remains slightly above the free-stream level in this example.

Figures 8(*a*) and 8(*b*) present the corresponding results for a thicker profile, $\tilde{\tau} = 0.373$ and $\tilde{\tau} = 0.45$ respectively, showing a rather different behaviour with respect to incidence change. The wake shortens instead of lengthens with increasing α/τ, approaching closely to the trailing edges ($x = 1$) at $\alpha/\tau = 0.419$ for $\tilde{\tau} = 0.373$, and at $\alpha/\tau = 0.284$ for $\tilde{\tau} = 0.45$. The breakaway location on the top surface s_1 also moves toward the trailing edge for increasing α/τ, while the location s_2 on the lower side moves forward. Another feature differing from figure 7 is the noticeably higher eddy pressure level as indicated by $-u_c$, and its variation with the angle of attack for these two cases.

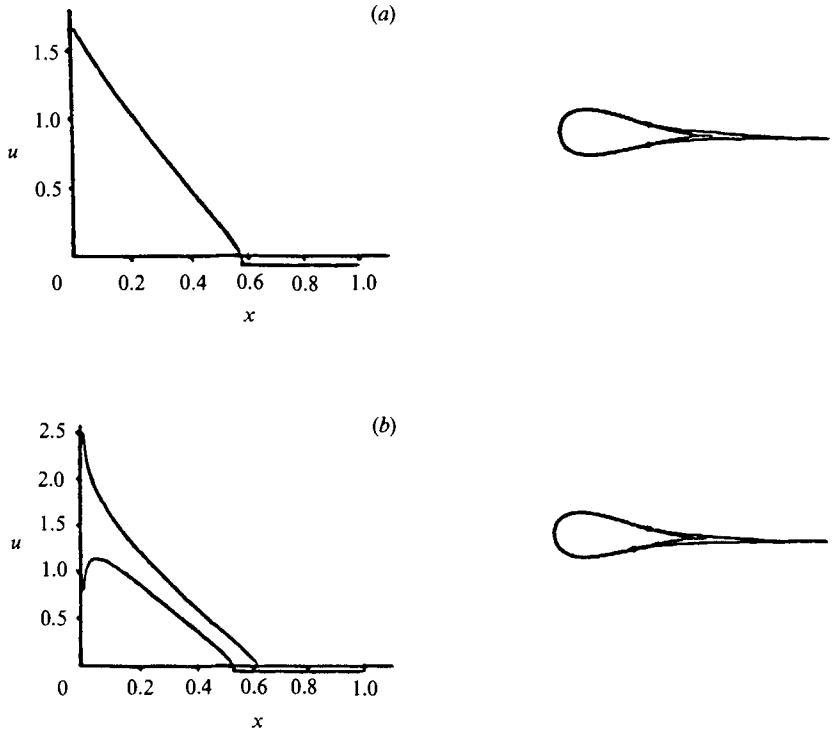

FIGURE 9(*a*,*b*). For caption see facing page.

4.4.2. *Surface pressure, wake shape, and the boundary layer*

As noted earlier, it is essential to ascertain that the breakaway streamlines do not intersect the surface in this case and that the boundary layer under the adverse pressure gradient remains attached upstream of the triple decks. With this in mind, the surface pressure and wake shape are computed from data based on the closed-wake solution for the body-scale flow, and shown in figure 9(*a–e*) for the model airfoil with $\tilde{\tau} = 0.20$ for four values of α/τ; $\alpha/\tau = 0$, 0.0873, 0.1571 and 0.2094. The closed-wake model with $\alpha/\tau = 0.2094$ yields two solutions consistent with the bifurcated range indicated earlier for this case (see figure 7).

Each breakaway streamline in figure 9(*a–e*) is seen to leave the surface smoothly and to not intersect or touch the surface a second time; the upper and lower streamlines meet downstream tangentially in the form of a cusp, as required. The surface pressure (or the surface u) distribution exhibits the required square-root singularities at the breakaway locations for the body-scale flow. The large adverse gradients next to the leading edge were an exaggeration resulting from the local breakdown (non-uniformity) of the linearization discussed earlier. Interestingly, not only is the wake in the upper-branch solution for $\alpha/\tau = 0.2094$ rather long ($l = 5.179$), approaching a Kirchhoff description, but the corresponding wake pressure also recovers close to the value stipulated in the Kirchhoff model ($u_c = 0$). Results similar to those of figure 9(*a–e*) have also been obtained for the thicker profiles with $\tilde{\tau} = 0.373$ and 0.45. They are omitted to conserve space, except for the breakaway streamlines in figure 10(*a*) which are shown for $\tilde{\tau} = 0.373$ at $\alpha/\tau = 0.4189$ corresponding to a branch point and in figure 10(*b*) for $\tilde{\tau} = 0.45$ at $\alpha/\tau = 0.2836$ which is also a branch point. The results suggest that they could be continued for α/τ

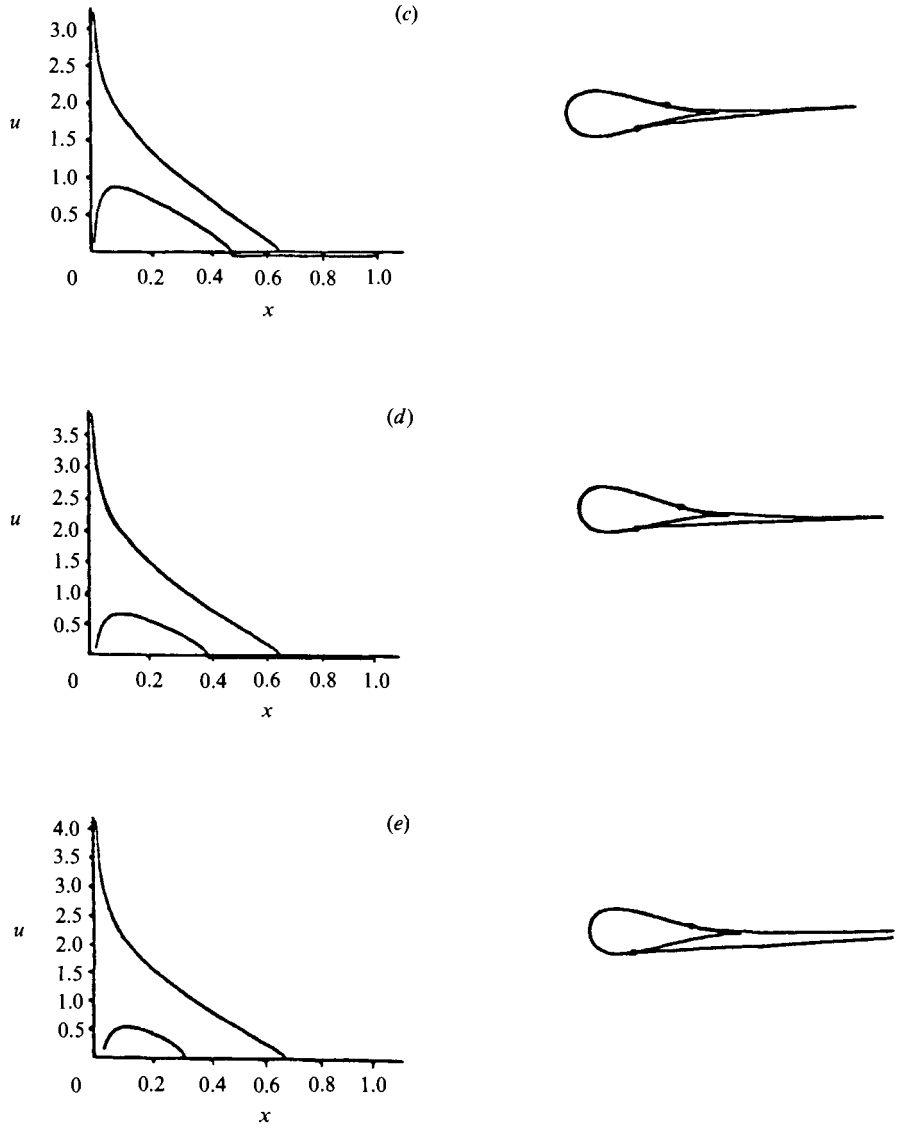

FIGURE 9. Breakaway streamlines and normalized surface pressure, u, over a model Joukowski airfoil of reduced thickness $\tilde{\tau} = 0.2$ according to a closed-wake solution at four different angles of attack: (*a*) $\alpha/\tau = 0$, $C_L/t = 0$; (*b*) $\alpha/\tau = 0.0873$, $C_L/t = 0.5105$; (*c*) $\alpha/\tau = 0.1571$, $C_L/t = 0.9400$; (*d*) $\alpha/\tau = 0.2094$, $C_L/t = 1.3206$; (*e*) $\alpha/\tau = 0.2094$, $C_L/t = 1.5346$. Note that (*d*) and (*e*) belong to different branches of the closed-wake solution and that the airfoil ordinates shown have been roughly doubled in order to exhibit more clearly the streamline geometry.

beyond the indicated value in a form belonging to the type (*c*), with a single eddy on the wing for $\tilde{\tau} = 0.373$, and with two eddies on the wing for $\tilde{\tau} = 0.45$, while the reattachments occur near $x = 1$. Figures 10(*a*) and 10(*b*) suggest that a rather long shallow bubble would appear on the lower side of the airfoil anterior to the trailing edge.

For type (*b*) closed wakes, symmetry breaking is not found at $\alpha = 0$, but these solutions obtained for $\tilde{\tau} = 0.20$ appear to match well with the upper solution branch of the type (*a*) open wake which break the flow symmetry at zero incidence. The good

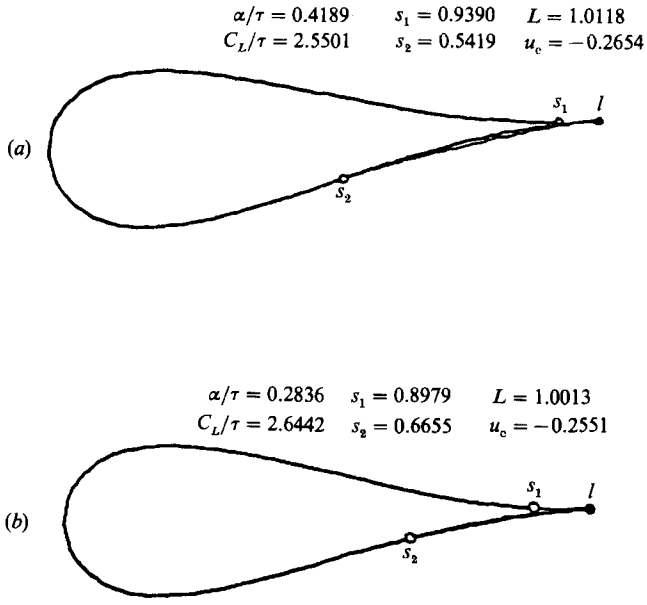

FIGURE 10. The streamlines on a closed wake leaving the model Joukowski airfoil of reduced thickness (*a*) $\tilde{\tau} = 0.373$ at an angle of attack corresponding to $\alpha/\tau = 0.4189$, and (*b*) $\tilde{\tau} = 0.45$ at an $\alpha/\tau = 0.2836$.

match between types (*a*) and (*b*) will be seen more clearly in a study of C_L *vs.* α. To ascertain the existence of a fully attached boundary layer upstream of the triple deck, a solution could be obtained numerically by integrating the parabolic boundary-layer equation with the surface pressure data shown in figure 9(*a–e*). Instead, the shape factor 'λ' (not to be confused with λ in (2.2), (2.3)) or 'K' in the classical integral method (Schlichting 1979) has been computed as function of x in the course of this study for each of figures 9(*a*)–9(*e*); this may suffice for the present purpose, as long as the λ or K so computed is not too close to its critical value for separation. According to Thwaites (1960), separation is anticipated at a location where K falls below -0.082, or below -0.1567, according to Holstein & Bohlen (1940). As noted earlier, the boundary-layer solution is controlled by the thickness ratio τ, not the reduced thickness ratio $\tilde{\tau}$; a $\tau = 0.112$ was therefore chosen for the computation of K, which corresponds to $Re = 10^4$ for $\tilde{\tau} = 0.20$. The chordwise distributions of the shape factor K computed is not presented here, to conserve space, but it should be mentioned that, in spite of the high adverse gradient at $x = 0$ and at s_1 and s_2, the shape factor k never falls below -0.082, corresponding to separation in each case tested. The lowest K value reached (at the breakaway) is typically -0.06, indicating attached boundary layers upstream of s_1 and s_2 in all cases examined.

4.5. *Bifurcation of steady-state lift*

The foregoing analysis is best summarized in terms of the lift and angle of attack, or more precisely, C_L/τ *vs.* α/τ, for a fixed $\tilde{\tau} \equiv Re^{\frac{1}{16}}\tau$, where the multiplicity of the steady states represented by different wake configurations as well as the bifurcation of the open- and closed-wake solutions themselves can be simultaneously studied.

An example is given in figure 11 for the reduced thickness ratio $\tilde{\tau} = 0.20$, where the upper and lower branches for type (*a*) open wakes are shown as (thin) solid curves, the central branch of type (*a*) is shown in (thin) dashes, and the type (*b*) closed-wake

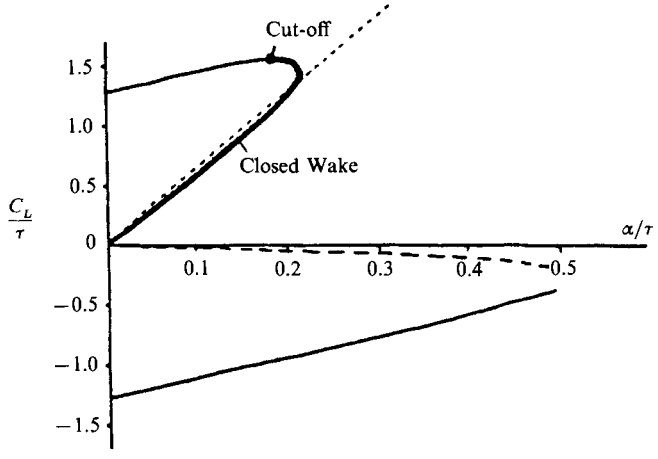

FIGURE 11. Alternative steady-state lift of a model Joukowski airfoil of reduced thickness $\tilde{\tau} = 0.2$ as a function of incidence-to-thickness ratio according to solutions from the upper and lower branches for open wakes (solid curve); from the central branch for open wakes (dashed); from the upper and lower branches for closed wakes (heavy solid curve); and the fully attached flow (dotted line).

solution (branch) is shown as heavy solid curve. The C_L/τ in the negative α/τ range (not shown) is simply that presented in figure 11 with the algebraic signs of C_L and α changed. Whereas the closed-wake branch cannot support symmetry breaking in this case, it connects up with the symmetry-breaking, upper open-wake branch at the cut-off value of α/τ for the Kirchhoff wake (see figure 11). The lower open-wake branch with negative lift is seen to merge with the central open-wake branch at a small negative C_L/τ near $\alpha/\tau = 0.50$ where a noticeable gap is left, however, by the computation in the right lower quadrant; whether changing over to other wake/eddy configurations would fill this gap is uncertain.

Accepting the fully attached flow as another admissible solution for a sufficiently thin airfoil at small enough incidence (for the reason given earlier), figure 11 then furnishes three positive and two negative (alternative) values of lift in the attack angle range $0 < \alpha/\tau \leqslant 0.22$, and one positive and two negative lift values in $0.22 \leqslant \alpha/\tau \leqslant 0.53$. The dotted line has the ideal slope 2π and corresponds to a fully attached flow according to the thin-airfoil theory. The presence of a closed-wake branch signifies that there will be at least one steady state involving laminar breakaway, in which, by virtue of its closed wake, the inviscid (pressure) drag is reduced to zero as for a fully attached flow. The slope $\mathrm{d}C_L/\mathrm{d}\alpha$ of the closed-wake solution turns out to be surprisingly close to 2π. The upper and lower open-wake branches represent a continuation of the two symmetry-breaking stages into the domain of $\alpha \neq 0$; as such, it signifies that the solution pair at $\alpha = 0$ is not isolated and has a rather extensive neighbourhood. Unlike the central open-wake branch, the incidence response, $\mathrm{d}C_L/\mathrm{d}\alpha$, in these two branches (though small) is by no means totally lost.

As one follows the upper open-wake branch and passes the cut-off point into the upper closed-wake branch in the direction of increasing α/τ, a pressure drag reduction is anticipated (if the steady state can be realized), while the lift is found to decrease slightly, and soon a branch point is reached at $\alpha/\tau \approx 0.22$, from which a smooth continuation on the (lower) closed-wake branch can be achieved only by reducing α/τ; a continued increase of α/τ beyond 0.22 can result only in jumping off

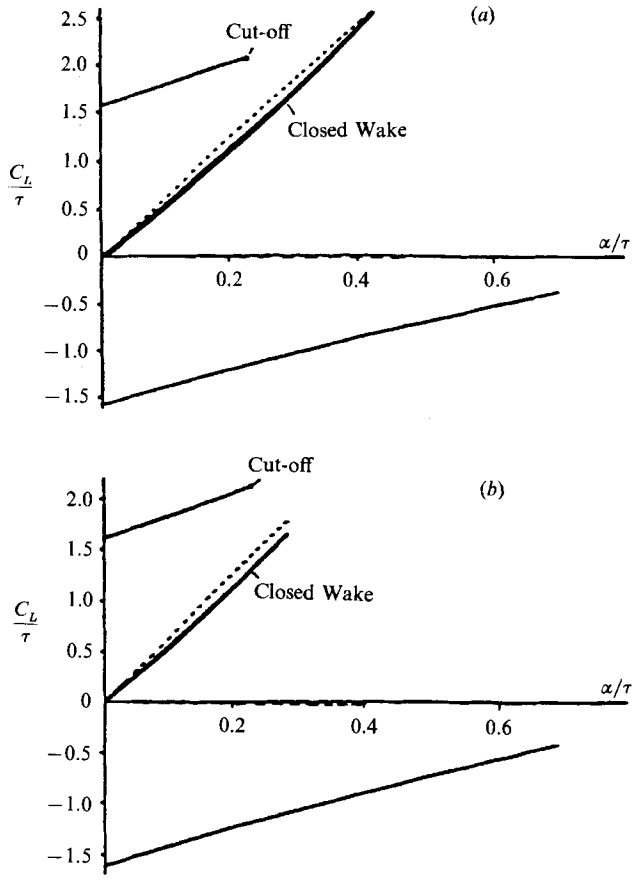

FIGURE 12. Alternative steady-state lift of a model Joukowski airfoil of reduced thickness (*a*) $\tilde{\tau} = 0.373$, and (*b*) $\tilde{\tau} = 0.45$ as a function of incidence-to-thickness ratio according to solutions from the upper and lower branches for open wakes (solid curve); from the central branch for open wakes (dashes), from the closed wake (heavy solid curve); and the fully attached flow (dotted line).

either to the other branches or to the fully attached solution (the dotted line). If the central branch proves to be (dynamically) unstable, the transition to the lower branch would involve a drop from the high-lift (closed-wake) branch to the lower-lift (open-wake) branch. This would constitute a part of the clockwise hysteresis loop, provided the two branches in question are stable, or more appropriately, *bistable* (borrowing the language of Schewe 1983). The foregoing description has thus furnished a few more details (for $\tilde{\tau} = 0.20$) about the scenario of such a transition. It would accordingly involve a wake shortening and a gradual lift reduction before a drastic reversal of lift direction. In the meantime, a scenario of switching from one stable state to another at any α/τ in response to external excitations may likewise be envisioned. The ranges of α allowed by $0 < |\alpha/\tau| < 0.22$ for $\tilde{\tau} = 0.20$ is rather limited, however, being comparable to $|\alpha| \leqslant 1°$ for a $\tau = 0.10$. The variety in the incidence response demonstrated here may nevertheless be compared with the anomalous behaviour (and the uncertain nature) found near zero lift recorded for NACA 0012 at $Re = 4 \times 10^4$–8×10^4 in Althaus' (1980) experiment.

Corresponding plots of C_L/τ *vs.* α/τ for the thicker profiles, $\tilde{\tau} = 0.373$ and 0.45, are shown in figures 12(*a*) and 12(*b*). These closed-wake solutions cannot be connected

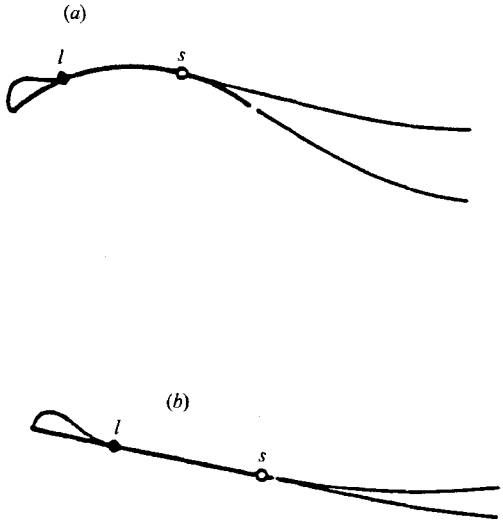

FIGURE 13. (*a*) Model of a subcritical body-scale flow about a single-surface airfoil with a leading-edge bubble and an open wake with one laminar-breakaway point on the upper surface. (*b*) Model of a subcritical body-scale flow of an inclined flat plate.

(continuously) with the open-wake solution at the 'cut-off' as it was for $\tilde{\tau} = 0.20$ in figure 11, owing to the convergence of the closure point to the trailing edge ($x = 1$) for α/τ increasing beyond 0.419 and 0.284 (see figures 8*a* and 8*b*). The model of type (*c*) is apparently a candidate for such a continuation, as noted earlier. In view of the cut-off occurring in the upper open-wake branch in these cases, there may exist other closed-wake solutions which serve as the continuation of the open-wake. The lift for the central branch (shown in dashes) is found to be practically zero with $C_L/\tau \leqslant 0.02$.

5. The single-surface airfoil

5.1. *Indeterminacy of a type (d) flow*

A simplified version of type (*d*) flow is represented by a cambered airfoil of zero thickness, commonly referred to as the 'single-surface airfoil', shown in figure 13(*a*). In this case, the eddy can be assumed to break away right at the leading edge ($x = 0$) and, for simplicity, a fully attached boundary layer is assumed on the concave, lower side. The latter assumption necessarily places a restriction on the lower limit of incidence range. With this restriction, the analysis reduces (see §3.5) essentially to the determination of three unknowns, namely the reattachment location l and the second breakaway location s and the eddy pressure $-u_c$ (see figure 13*a*). The criterion (3.5) is not needed at the known breakaway point ($x = 0$), and is applied only at the second breakaway location ($x = s$). As indicated in §3, a complete determination of this steady body-scale flow is lacking; an additional condition, such as a specification of the eddy pressure, is required for the final solution.

This description includes the flat plate at incidence (figure 13*b*) as a special case and, as such, is theoretically interesting in that the open wake in this type of flow may now account for the pressure drag which is roughly the incidence angle multiplied by the lift. A peculiar feature of this model is that even if the boundary layers on both sides of the plate were to remain fully attached, i.e. $s = 1$, the open wake cannot be made to vanish and the indeterminacy would still remain. The flow

structure resembles in certain aspects the single-burbling theory of Witoszynski & Thompson (1934). If the breakaway were assumed to occur at a $x = s$ upstream of the trailing edge, which is close enough to the trailing edge that $(1-s)$ is small compared to unity but large compared to the triple-deck width (ϵ^3), this indeterminacy may be eliminated. With this stipulation, and a provisional value of $\lambda \approx 0.332$ (cf. the earlier discussion on type (*d*) flow in §3.5), the lift on a flat plate at small and moderate attack angles can be obtained as a function of the attack angle; the values turn out to be comparable to Schmitz's (1942) data for $Re = 10^4$–10^5 below stall. Such a description must be viewed as being *ad hoc*, however.

In passing, we note that for a cambered airfoil which is not so thin ($\tau \neq 0$), there is a critical attack angle for the breakdown of the attached boundary layer over the leading-edge region (Lighthill 1951; also Smith & Elliot 1985). However, for the type of single-surface airfoil considered here and below, the τ, if any, is supposed to be negligibly small compared to σ, and the breakdown mentioned can raise the critical value of α/σ for a shock-free entry only slightly.

5.2. *The circular-arc airfoil with shock-free entry*

A much greater simplification of the single-surface airfoil problem occurs when the angle of attack is so adjusted as to eliminate the leading-edge bubble completely; the problem is degenerated to that of type (*a*) open wake. The analysis in this case (with fuller details presented in Cheng 1984) provides a compact data set which should be useful for performance analyses of avian/insect flight. This corresponds to a 'shock-free entry' for fluid particles riding along a streamline which wets the airfoil surface. As is well known, the angle of attack α for a circular-arc, zero-thickness airfoil at which the shock-free entry occurs is $\alpha \equiv 0$ according to the classical thin-airfoil theory (Munk 1924; Kármán & Burger 1934). For the slightly viscous flow considered here, this angle has to be raised because the breakaway occurs on the top surface. For this case, an analytic solution for the breakaway location s can be obtained for each reduced camber $\tilde{\sigma} \equiv Re^{\frac{1}{16}}\sigma$. Unlike the multitude of solutions in most other examples, the results of the breakaway location s, and related characteristics in this special case are *unique*, *monotone* functions of the reduced camber $\tilde{\sigma}$. Results for s, α/σ, lift, drag and centre of pressure (taken from Cheng 1984) are presented in figure 14(*a*, *b*) as functions of $\tilde{\sigma}$. All properties shown in figure 14(*b*) are surprisingly insensitive to a change in $\tilde{\sigma}$ as long as $\tilde{\sigma} \geqslant 0.35$ – a fact useful for performance analyses for this flight regime. The (pressure) drag vanishes when the body-scale flow becomes fully attached and this occurs at a range of finite (though numerically small) $\tilde{\sigma} \leqslant 0.08$, or $\tilde{\alpha} \leqslant 0.027$. This would appear to agree with the trend anticipated from Smith's (1983) trailing-edge stall study cited earlier (§2.2), according to which the point of zero wall shear in the lower deck can move upstream away from the trailing edge.

These results should be of considerable interest to students of insect/avian flight, as well as swimming propulsion of animals, not only for their realizable Re-range (10^3–10^5), but for the reasonable hydrodynamic performance and stability characteristics achievable by a moderate camber σ. With a $\sigma \equiv Re^{-\frac{1}{16}}\tilde{\sigma} \geqslant 0.35Re^{-\frac{1}{4}}$ (cf. figure 14*a*, *b*), one can base the analysis on the simple formula $C_L \approx 1.76\sigma$ and $C_D = C_{D_0} + 0.136C_L^2$. Hence, a unit-order lift coefficient and an optimum lift/drag ratio in the range 5–10 are attainable even in the presence of massive flow separation in this case. (Note, the maximum camber height of this airfoil is $\frac{1}{4}\sigma$.) Equally attractive are perhaps the almost universal centre of pressure location, $\bar{x}_{cp}$, and the trim incidence angle, $\tilde{\alpha} \equiv \alpha/\sigma = 1/3$. which are affected little by the Reynolds number.

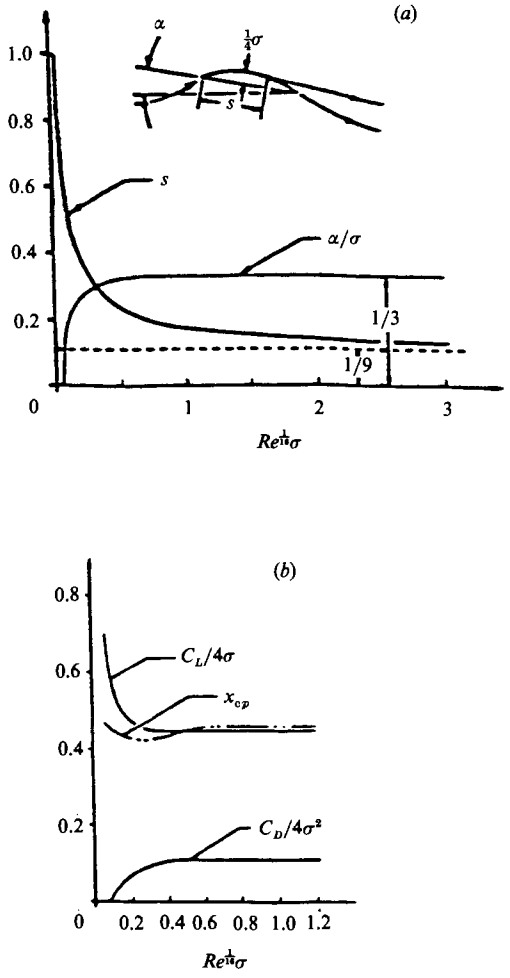

FIGURE 14. (*a*) Breakaway location and incidence angle of a single-surface, circular-arc airfoil for a smooth shock-free entry as a function of reduced camber $\tilde{\sigma} \equiv Re^{\frac{1}{16}}\sigma$. (*b*) Normalized lift, centre-of-pressure location and drag for the same airfoil as a function of reduced camber (from Cheng 1984).

6. Discussion

In the foregoing study, we have examined several examples of steady-flow models of laminar breakaway for airfoils with thickness, incidence or camber of order $\epsilon^{\frac{1}{2}}$, i.e. $Re^{-\frac{1}{16}}$. Applying the triple-deck breakaway criterion and assuming a stagnant wake/eddy model, multiple steady states representing body-scale flows with open and closed wakes and other eddy configurations are found to be admissible in certain parts of the unit-order $\tau\epsilon^{-\frac{1}{2}}$ domain. In the (parameter) domain where the boundary-layer approximation holds uniformly (in space), the study indicates that it may not be the only self-consistent description of the global flow in a steady state. These solution bifurcations suggest that lift hysteresis, symmetry breaking and other forms of anomalies can also occur in purely laminar steady flows. The paper summarizes and extends an earlier development (Cheng & Smith 1982; Cheng 1984, 1985; Cheng & Lee 1985) to allow a finite wake. As demonstrated by the example, the transition from an open-wake solution to one with a closed wake need not be abrupt, in which

the Kirchhoff model with $p_c = p_\infty$ can be recovered and approached asymptotically from a closed-wake model.

The most serious limitation of the present analysis from the viewpoint of flow physics is the steady-state assumption; this, together with the complexities and subtlety of the various issues, makes the significance of the results lie more, perhaps, in what they suggest than in themselves. The solutions and their qualitative features may best be viewed as useful conjectures towards better model construction. The bifurcation features have brought out quite clearly the need for an examination of their instability and their physical relevance. This need is presumably more critical for flow in the high subcritical Re-range (say $Re \sim 10^5$–10^6). If more than one of these multiple states is proved to be stable, the large-time behaviour of interest must depend on the initial conditions and the evolution history that follows; the dynamical models and computation programs used to assess the flow behaviour in question must therefore be time-accurate. Nevertheless, the many CFD codes with artifices for accelerating convergence to the steady state could also be helpful to this type of study, inasmuch as they may add or suggest new members to the multiple steady-state solutions not accessible via the present approach. One may caution, however, that certain algorithms used, as well as certain symmetry properties implicit in the computation, could very well dictate a preferred choice for certain steady states.

The time-dependent aspect not treated here will be important not only for the flow instability consideration but also with regards to the possibility of arriving at a meaningful long-time-averaged description for the nonlinear body-scale flow, which often exhibits hysteresis, symmetry breaking and other anomalies. In passing, we note that, for most unsteady body-scale flows of aerodynamic interest, the characteristic timescale is an order ϵ^{-2} longer than the flow transit time of the triple deck which may thus be treated as being quasi-steady, leaving the Sychev criterion (2.3) for the steady state unchanged.

Whereas the definition of the triple-deck interaction parameter $\tilde{\tau} \equiv \tau Re^{\frac{1}{16}}$ would indicate a relatively insensitive dependence on the Reynolds number, a strong Re-dependence is expected in the vicinity of critical values of $\tilde{\tau}$ corresponding to branch points and cut-off points where the steady-state flow structure changes branch/type. Therefore, the degree of Re-dependence is non-uniform and becomes more critical near a singularity in the parametric domain of the steady-state solution. Computational and laboratory experiments designed to verify the significance of this parameter and flow sensitivity to Re-changes should pay attention to the existence of these critical values of the reduced thickness or incidence.

The support by the Office of Naval Research under contract N00014-82-K-0315 throughout the entire course of this study is gratefully acknowledged. Helpful discussion with Professors S. N. Brown, P. Huerre, and F. T. Smith are very much appreciated. Our thanks are due also to Dr H. Werlé for providing the glossy print of the photo records used in figure 2.

REFERENCES

ALTHAUS, D. 1980 *Profilpolaren für den Modellflug: Wind Kanalmessungen an Profilen im Kritischen Reynoldszahlbereich.* Neckar-Verlag Vs-Villingen.

ASHLEY, H. & LANDAHL, M. 1965 *Aerodynamics of Wings and Bodies.* Addison-Wesley.

BATCHELOR, G. K. 1967 *An Introduction to Fluid Dynamics*, p. 504. Cambridge University Press.

BRODETSKY, S. 1923 *Proc. R. Soc. Lond.* A **102**, 542.

BROWN, S. N., CHENG, H. K. & SMITH, F. T. 1988 *J. Fluid Mech.* **193**, 191.

BROWN, S. N. & STEWARTSON, K. S. 1970 *J. Fluid Mech.* **42**, 561.

CARLEMAN, T. 1922 *Arkiv för Matematik och Fysik* **16**, 26.

CARMICHAEL, B. H. 1981 *NACA-CR* 165803.

CEBECI, T., STEWARTSON, K. & WILLIAMS, P. G. 1980 *AGARD CP-291 Paper* 20.

CHENG, H. K. 1984 *AIAA Paper* 84-1612; superseded by *USCAE Rep.* 141 (1985).

CHENG, H. K. 1985 In *Proc. Conf. Low Reynolds Number Airfoil Aerodynamics. Univ. Notre Dame.* (ed. T. J. Mueller). *UNDAS-CP* 7712123.

CHENG, H. K. 1986 On massive laminar separation and lift anomalies in subcritical *Re*-range. *Proc. Intl Conf. Aerodynamics at Low Reynolds Number*, 16–17 October 1986. London: Royal Aeronautical Society.

CHENG, H. K. & LEE, C. J. 1985 *Proc. 3rd Symp. Numerical & Physical Aspects of Aerodynamic Flows.* Springer.

CHENG, H. K. & ROTT, N. 1954 *J. Rat. Mech. Anal.* **3**, no. 3.

CHENG, H. K. & SMITH, F. T. 1982 *Z. Angew. Math. Phys.* **33**, 151.

DANIELS, P. G. 1979 *J. Fluid Mech.* **90**, 289.

ELLIOT, J. W. & SMITH, F. T. 1987 *J. Fluid Mech.* **179**, 489.

EPPLER, R. 1978 *NASA TM* 75328 (transl. from *Ing.-Arch.* **32**, 1963).

FORNBERG, B. 1980 *J. Fluid Mech.* **98**, 819.

FORNBERG, B. 1985 *J. Comput. Phys.* **61**, 297.

GASTER, M. 1967 *Aero. Res. Counc. R & M* 3595.

GLAUERT, H. 1926 *Aero. Res. Counc. R & M* 910.

GOLDSTEIN, M. E. 1984 *J. Fluid Mech.* **145**, 71.

GOLDSTEIN, S. 1948 *Q. J. Mech. Appl. Maths* **1**, 43.

HOLSTEIN, H. & BOHLEN, T. 1940 *Lilienthal-Bericht* S10, 5.

JOOSE, G. & JOSEPH, D. D. 1980 *Elementary Stability and Bifurcation Theory.* Springer.

KÁRMÁN, TH. VON & BURGERS, J. M. 1934 General aerodynamics theory – perfect fluids. In *Aerodynamic Theory Vol. II, Div. E* (ed. N. F. Durand), pp. 48–53. Durand Reprinting Committee, California Institute of Technology.

KIRCHHOFF, G. 1869 *J. Reine Angew. Math.* **70**, 289.

KOROLEV, G. L. 1980 *Sci. J. TSAG.*, XI, No. 2, 27.

LAMB, H. 1932 *Hydrodynamics.* Cambridge University Press.

LEE, C. J. 1988 A study of laminar separation from a thin obstacle. Ph.D. thesis, University of Southern California.

LIEBECK, R. H. 1973 *J. Aircraft* **10**, no. 10, 610.

LIGHTHILL, M. J. 1949 *Aero. Res. Council R & M* 2328.

LIGHTHILL, M. J. 1951 *Aero. Q.* **3**, 193.

LISSAMAN, P. B. S. 1983 *Ann. Rev. Fluid Mech.* **15**, 223.

LOCK, R. C. 1951 *Q. J Mech. Appl. Maths* **4**, 42.

MELNIK, R. E. & CHOW, R. 1975 *Grumman Res. Rep.* Re-510 J.

MESSITER, A. F. 1970 *SIAM J. Appl. Maths* **18**, 241.

MESSITER, A. F. 1978 *Proc. 8th US Natl Appl. Mech. Cong., Los Angeles, CA.*

MESSITER, A. F. 1983 *J. Appl. Mech.* **50**, 1104.

MORKOVIN, M. & PARANJAPE, S. V. 1971 *Z. Flugwiss.* **9**, 328.

MUELLER, T. J. 1979 *Agardograph* 288.

MUELLER, T. J. 1985 *Proc. Conf. Low Reynolds Number Airfoil Aerodynamics, Univ. Notre Dame*, UNDAS-CP 7713123.

MUNK, M. M. 1924 *NACA Rep.* 191.

NEILAND, V. YA. 1969 *Izv. Akad. Nauk. SSSR Mekh Zhid Gaza* **4**.

PEREGRINE, D. H. 1985 *J. Fluid Mech.* **157**, 493.

ROTHMAYER, A. P. & DAVIS, R. T. 1985 In *Proc. Symp. on Vortex Dominated Flows* (ed. M. Y. Hussaini & M. D. Salas). Springer.

RUBAN, A. I. & SYCHEV, V. V. 1979 *Adv. Mech.* **2**, 57.

SADOVSKII, V. S. 1971 *Appl. Math. Mech.* **35**, 729 (transl. from *Prikl. Math. Mech.* **35**, 773).

SCHEWE, G. 1983 *J. Fluid Mech.* **133**, 265.

SCHLICHTING, H. 1979 *Boundary-Layer Theory.* McGraw Hill.

SCHMITZ, F. W. 1942 *Aerodynamics Des Flugnodells, Trag-flügel, Messungen I.* Berlin-Charlottenburg 2: C. J. E. Volckmann Nachf. E. Wette.

SEDOV, L. I. 1965 *Two-Dimensional Problems in Hydrodynamics and Aerodynamics.* International Science Publications.

SMITH, F. T. 1977 *Proc. R. Soc. Lond.* A **356**, 443.

SMITH, F. T. 1979 *J. Fluid Mech.* **92**, 171.

SMITH, F. T. 1982 *IMA J. Appl. Maths* **28**, 207.

SMITH, F. T. 1983 *J. Fluid Mech.* **131**, 219.

SMITH, F. T. 1985 *J. Fluid Mech.* **155**, 175.

SMITH, F. T. 1986 *Ann. Rev. Fluid Mech.* **18**, 197.

SMITH, F. T. & ELLIOT, J. W. 1985 *Proc. R. Soc. Lond.* A **401**, 1.

SOUTHWELL, R. V. & VAISEY, G. 1946 *Phil. Trans. R. Soc. Lond.* A **240**, 177.

STEWARTSON, K. 1958 *Q. J. Mech. Appl. Maths* **11**, 397.

STEWARTSON, K. 1969 *Mathematica* **16**, 106.

STEWARTSON, K. 1974 *Adv. Appl. Math.* **14**, 145.

STEWARTSON, K. 1981 *SIAM Rev.* **23**, 308.

STEWARTSON, K., SMITH, F. T. & KAUP, K. 1982 *Stud. Appl. Maths* **67**, 45.

SYCHEV, V. V. 1972 *Izv. Akad. Nauk. SSSR Mekh. Zhid Gaza* **3**, 43.

SYCHEV, V. V. 1987 *Asymptotic Theory of Separated Flows.* Moscow: Nauka.

TANI, I. 1964 *Prog. Aero. Sci.* **5**, 70.

THWAITES, B. 1960 *Aero. Q. J.* **1**, 245.

VAN DOMMELEN, L. L. & SHEN, S. F. 1983 *Proc. 2nd Symp. Numerical and Physical Aspects of Aerodynamic Flows, Calif. State Univ., Long Beach, CA*, section 2. Springer.

VAN DYKE, M. D. 1975 *Perturbation Methods in Fluid Mechanics.* Parabolic.

VAN DYKE, M. D. 1982 *An Album of Fluid Motion*, pp. 19, 25, 26. Parabolic.

WERLÉ, H. 1974 *ONERA Pub.* 156.

WITOSZYNSKI, C. & THOMPSON, M. J. 1934 The theory of single burbling. In *Aerodynamic Theory*, vol. III, Div. F (ed. W. F. Durand), p. 1. Durand Reprinting Committee, California Institute of Technology.

WU, T. Y. T. 1972 *Ann. Rev. Fluid Mech.* **4**, 243.